

Published in final edited form as:

*Chem Soc Rev.* 2013 April 7; 42(7): 2725–2745. doi:10.1039/c2cs35365b.

## From the Bottom Up: Dimensional Control and Characterization in Molecular Monolayers†

Shelley A. Claridge<sup>1,2</sup>, Wei-Ssu Liao<sup>1,2</sup>, John C. Thomas<sup>1,2</sup>, Yuxi Zhao<sup>1,2</sup>, Huan Cao<sup>1,2</sup>, Sarawut Cheunkar<sup>1,2</sup>, Andrew C. Serino<sup>1,2</sup>, Anne M. Andrews<sup>1,2,3,4</sup>, and Paul S. Weiss<sup>1,2,5,\*</sup>

<sup>1</sup>California NanoSystems Institute, University of California, Los Angeles, Los Angeles, California 90095, United States

<sup>2</sup>Department of Chemistry & Biochemistry, University of California, Los Angeles, Los Angeles, California 90095, United States

<sup>3</sup>Department of Psychiatry, University of California, Los Angeles, Los Angeles, California 90095, United States

<sup>4</sup>Semel Institute for Neuroscience & Human Behavior, University of California, Los Angeles, Los Angeles, California 90095, United States

<sup>5</sup>Department of Materials Science & Engineering, University of California, Los Angeles, Los Angeles, California 90095, United States

### Abstract

Self-assembled monolayers are a unique class of nanostructured materials, with properties determined by their molecular lattice structures, as well as the interfaces with their substrates and environments. As with other nanostructured materials, defects and dimensionality play important roles in the physical, chemical, and biological properties of the monolayers. In this review, we discuss monolayer structures ranging from surfaces (two-dimensional) down to single molecules (zero-dimensional), with a focus on applications of each type of structure, and on techniques that enable characterization of monolayer physical properties down to the single-molecule scale.

### 1. Introduction

The unique chemistry of nanostructured materials evolves due to balance between the lattice and bonding structures of the materials, the chemistries of their interfaces, the dimensionalities of their structures, and the types and distributions of defects (Figure 1). In comparison with other nanoscale materials, the chemistries and structures of self-assembled monolayers (SAMs) are largely determined by their interfaces, which account for a relatively high proportion of the atoms (typical monolayer thickness ranges from 1–3 nm<sup>1</sup>), and also frequently dominate the energetics of structure formation. For instance, in the most common synthetic SAMs, alkanethiols on gold, the enthalpy of the gold–sulfur bond formation (~50 kcal/mol)<sup>2</sup> is several times larger than the combined interactions of the alkyl tails with surrounding molecules (1–2 kcal/mol·CH<sub>2</sub>).<sup>3</sup> Importantly, if the enthalpy of assembly at one interface provides a strong driving force for monolayer formation, it is possible to tune many other material properties and still achieve ordered lattices.

†Part of the chemistry of functional nanomaterials themed issue.

\*To whom correspondence should be addressed: psw@cnsi.ucla.edu (P.S.W.).

Monolayer structures optimize both interactions with the substrate and intermolecular interactions.<sup>1,4-6</sup> Lattice structures in monolayers are determined by both the substrate lattice and the chemistries and structures of the molecules forming the monolayers. In alkanethiol monolayers, linear molecules are attached to gold surfaces via Au–S bonds; both the organization of the sulfur headgroups on the gold lattice and the packing of the alkyl tails influence molecular lattice formation. For other molecules, such as adamantanethiols and carboranethiols, the tails are bulkier than the headgroups, and can play larger roles in lattice formation.<sup>6</sup> In still other monolayers, such as those formed based on noncovalent interactions with graphite, molecules lie down, maximizing their interactions with the substrate.<sup>4</sup>

Although monolayers are typically considered to be two-dimensional (2D) structures, it is equally possible to assemble one-dimensional (1D) and zero-dimensional (0D) molecular structures on surfaces. As with nanocrystals, the definitions of dimensionality arise from the physical properties of interest in the structure – that is, anisotropic molecules that assemble across a 2D surface, but display strong directional coupling may be considered as 1D structures.<sup>7,8</sup> Similarly, individual functional molecules deposited on surfaces can act as 0D structures, with properties that can be controlled and measured individually.<sup>9,10</sup> Dimensionality at the molecular scale can also be combined with large-scale patterning processes such as soft lithography.<sup>1,11</sup>

Defects are important in understanding and predicting the behavior of monolayers.<sup>12</sup> Since monolayers are often tightly coupled to solid substrates, irregularities in the substrate lattices (such as atomic step edges) can create offsets in the monolayers.<sup>5</sup> Defects can also arise from the molecular lattices. For instance, many classes of molecules tilt relative to the surface normal,<sup>5</sup> creating areas of heterogeneous structure between domains of molecules oriented in different azimuthal directions. Still other defects can be created as monolayers are formed. When alkanethiols are assembled on gold from solution, thiols can extract gold atoms from the surface, resulting in one-atom-deep ‘etch pits’ in the Au{111} substrate surface that disrupt monolayer structures.<sup>5</sup> These and other defects can be selectively removed by subsequent monolayer and substrate dynamics and processing.<sup>13</sup>

Importantly, as with other nanostructured materials, defects are often the most reactive sites in the materials, and dominate both access of additional molecules to the substrates and the dynamics of the systems. In the context of monolayers, this reactivity can be exploited to design 1D and 0D structures within 2D monolayers, or to nucleate processes such as molecular exchange.<sup>14-20</sup>

Characterization of lattice structures and defects in SAMs and related structures relies on surface-sensitive tools that provide chemical, electronic, and/or topographic information.<sup>12,21</sup> Typical 2D techniques providing chemical information about surfaces and adsorbates include grazing angle Fourier transform infrared (FTIR) spectroscopy, Raman spectroscopy, electron diffraction (transmission electron microscopy, TEM, and low energy electron diffraction, LEED), near-edge X-ray absorption fine structure (NEXAFS), and neutron scattering.<sup>1</sup> Scanning probe techniques – atomic force microscopy (AFM) and scanning tunneling microscopy (STM) – provide more localized information, down to the single-molecule scale.<sup>21</sup> In this review, we discuss the physical properties and applications of self-assembled monolayers as nanostructured materials, with a focus on assembled structures ranging from 2D (full monolayers) down to 0D (single molecules), including methods for top-down patterning of monolayer structures. Throughout, we select examples highlighting the breadth of molecular functions available through these materials, and specialized characterization techniques and methods that enable quantitative measurements of these properties down to the single-molecule scale.

## 2. Two-dimensional structure and function

Studies of 2D monolayers on solid surfaces began as early as the 1940s,<sup>22</sup> and now encompass systems ranging from alkanes and aromatic molecules to much larger macromolecules, and substrates from glass to single-crystalline metal surfaces.<sup>1,4,23–25</sup> Self-assembled monolayer structure is influenced by the substrate lattice, the interface between the molecular head group functionality and the substrate, a molecular lattice formed based on head group and backbone chemistries, and an exposed interface dominated by the chemical functionality of the tail group (Figure 2). Monolayers of alkanethiols on Au{111} are the most common and most studied;<sup>1</sup> thus, we discuss many aspects of monolayer formation and structure in relation to these systems. The strategies developed for controlling monolayers of thiols on Au{111} will, over time, be translated to other molecule–substrate systems.<sup>6,26</sup>

### 2.1. Substrate lattices

Monolayers have been formed on metals including Au,<sup>1,12,27</sup> Ag,<sup>27–29</sup> Cu,<sup>27,30,31</sup> Pd,<sup>30,32</sup> Pt,<sup>33,34</sup> Ni,<sup>30,35</sup> Fe,<sup>30</sup> Ti,<sup>36</sup> Te,<sup>37</sup> Hg,<sup>38</sup> and GaIn.<sup>39,40</sup> Since bonding with the substrate is often a critical driving force for monolayer formation, the substrate atomic lattice and electronic structure are key. The Au{111} crystal face is often used in monolayer formation for a number of reasons—gold readily forms bonds with thiols, and such surfaces are easily formed, commercially available, and stable under normal atmospheric conditions. Other metal surfaces (such as Ag, Cu, Pt, and Pd) are more easily oxidized; these other substrates are often used in studies of monolayers under vacuum, in which molecules are evaporated onto the surface rather than deposited from solution.

Semiconductors such as Si, Ge, GaAs, and InP can also be used as substrates for monolayer formation.<sup>41–46</sup> Silicon is particularly widely used due to its electronic applications; however, silicon forms a native oxide under normal atmospheric conditions. Thus, chemistry has developed to interface with both silicon and its oxide.<sup>47–49</sup> Other semiconductors have also been explored as monolayer substrates, including GaN<sup>50</sup> and ZnSe.<sup>51</sup>

Highly oriented pyrolytic graphite (HOPG) is a semimetal and forms atomically flat surfaces over relatively large areas (>1000 nm on an edge). Although the surface does not readily form covalent bonds to common functional groups such as thiols or amines, it can be used as a substrate for monolayers in which aromatic groups in the monolayers form  $\pi$ -stacking interactions with graphite (or graphene) surfaces.<sup>4,52–55</sup>

### 2.2. Substrate-head-group interfaces

The substrate–molecule interface influences both monolayer structures and serves as the electronic connection to the substrate. Thus, understanding these interfaces is important in predicting structures, stabilities, and physical properties (such as conductance) of SAMs, as well as of molecules matrix-isolated within them.

Although there are many possible pairings of substrate and molecular head group chemistries, the substrate–molecule interface is more complex than would be predicted based solely on bonding between substrates and the functional head groups. The substrate lattice presents multiple chemically non-equivalent binding sites, involving one or more atoms. Further, substrate surfaces often reconstruct to minimize energy; these changes create lower symmetry surface structures that also influence the interfaces. Binding of the functional head group can lead to additional surface structural changes, and restrictions on orbital hybridization can influence the angle between molecular backbones and surfaces.

Surface reconstruction is widely observed for metal and semiconductor surfaces.<sup>56,57</sup> Here, we briefly discuss the relationship between surface reconstruction and alkanethiol SAM formation on Au{111} as an illustrative example of the complexities of these rearrangements.

Substrate atoms on bare Au{111} surfaces compact slightly, forming a reconstruction with both face-centered-cubic- and hexagonally close-packed-stacked zones and a (22× 3) unit cell relative to the Au{111} lattice, referred to as the herringbone reconstruction. When sulfur-containing molecules (including thiols, disulfides, and thioethers) bind to Au{111}, the formation of Au–S bonds removes the reconstruction, a phenomenon that is possible to visualize by STM. The nominal strength of Au–S bonds (~50 kcal/mol) is greater than that of Au–Au bonds,<sup>28,58</sup> and the ability to remove the reconstruction can be used as a qualitative descriptor of molecule–substrate bond strengths. For instance, thioethers have weaker molecule–substrate bonds than thiols; however, SAMs of thioethers nonetheless lift the Au{111} herringbone reconstruction.<sup>59–62</sup> In contrast, adsorbed benzene does not lift the native Au{111} reconstruction.<sup>63</sup>

The growing consensus is that thiols lift selected atoms to sit at a subset of sites on the restored Au{111} lattice; these are referred to as Au adatoms.<sup>64</sup> It has been known for some time that thiolates move as a Au-thiolate complex at defect sites such as step edges.<sup>65</sup> Recent calculations show that there are multiple stable surface reconstructions (similar to within 0.2 eV): one sulfur bound to a three-fold hollow site, one sulfur bound to a bridge site, one sulfur bound to one Au adatom, and two sulfur atoms bound to one Au adatom.<sup>66–71</sup> Thiols on Ag{111} exhibit different binding properties than those on Au{111},<sup>72</sup> typically binding at bridge and three-fold hollow sites, and are tilted at angles closer to the surface normal.<sup>29</sup> Selenols on Au{111} have more promiscuous binding, and as a result Moiré patterns are observed in STM images.<sup>73</sup>

The multiplicity of possible binding structures highlights the importance of techniques for characterizing the buried interfaces. Some chemical properties can be characterized at large (micron to millimeter) scales using techniques such as FTIR spectroscopy and X-ray photoelectron spectroscopy (XPS), or at intermediate scales by measuring reductive desorption electrochemically.<sup>20</sup> However, characterization at the sub-nanometer scale with STM-based techniques provides complementary information about heterogeneous structure important for understanding reconstructions. Weiss and coworkers found that the largest buried dipole in a SAM can be mapped by varying the tunneling gap distance in STM imaging. For alkanethiols on Au{111}, this locates the Au–S bond; thus, correlating buried dipoles (head groups) with topography (tail groups) enabled the first single-molecule tilt angle measurement.<sup>74</sup> A similar spectroscopy technique applied to cyclhexanethiol on Au{111} distinguishes between binding at bridge and atop sites.<sup>2,24,27</sup>

In addition to the molecules with head groups based on sulfur, discussed above,<sup>1,28,25</sup> many other head groups are available, including isocyanides,<sup>75</sup> Si,<sup>76–78</sup> P,<sup>50,79–81</sup> Se,<sup>29,73,82,83</sup> carboxylic acids,<sup>84,85</sup> and head groups that allow noncovalent  $\pi$ -stacking interactions on highly oriented graphite, such as cyclodextrins,<sup>86–89</sup> pentacene,<sup>90</sup> and peptides.<sup>91–93</sup> While these surface connectors are relatively less explored, comparisons between molecule–substrate systems provide insight into how to translate surface attachment and patterning strategies from one system to another, and will hopefully lead to the identification of new strategies.

Selenols provide a useful comparison with thiols since they come from the same group in the periodic table.<sup>83,94–96</sup> In contrast to the hexagonal lattices formed by alkanethiols, alkaneselenols form either densely packed distorted hexagonal lattices incommensurate with

the underlying Au{111} substrate, or commensurate linear missing-row structures.<sup>73</sup> These differences in bonding likely contribute to the differences in conductance observed between alkaneselenol and alkanethiol SAMs.<sup>97</sup> Short ( $n = 2-6$ ) *n*-alkaneselenols follow the odd/even rule for stability (even chain lengths are more stable), as do alkanethiols. However, selenols are more stable toward exchange than alkanethiols of equivalent length,<sup>98</sup> which has been attributed to differences in bonding configurations ( $sp^3$  and  $sp$ ).<sup>29</sup> Polyfunctional head groups increase binding strength; for instance, diselenides and dithiols displace monothiolate monolayers on Au, similar to chelating effects found for other molecules.<sup>94</sup>

Silanes and silanols are typically used to form monolayers on silica ( $SiO_2$ ) surfaces.<sup>25,99,100</sup> Head groups based on phosphorus (including phosphonates, phosphines, and phosphonic acids) are also common. Phosphorus headgroup binding on metals, such as Au, is generally weaker than thiol binding, but strong enough (in the case of trimethylphosphine) to lift the Au reconstruction.<sup>79</sup> Phosphonic acids form stable monolayers on Ti and Au substrates,<sup>36</sup> and phosphonates and alkylphosphonic acids assemble on GaN and nitinol (NiTi), respectively.<sup>50,101</sup> Alkylphosphonates assemble on  $Al_2O_3$ ,  $TiO_2$ ,  $ZrO_2$ , planar mica,  $TiO_2$  and  $SiO_2$ ,<sup>80</sup> however, monolayer structures are typically found to be less regular, and largely based on backbone and tailgroup interactions.

Monolayers can also form based on noncovalent interactions with substrates. Noncovalently bound molecular monolayers have been studied by STM, in many cases at low temperature, to stabilize the self-assembled structures sufficiently for imaging.<sup>102,103</sup> Many conjugated molecules can also form 2D assemblies on surfaces, including styrene,<sup>104</sup> pentacene,<sup>90</sup> pyrene,<sup>25</sup> and larger graphitic molecules.<sup>105,106</sup> Peptides can also assemble noncovalently on graphite surfaces, typically forming linear arrangements due to hydrogen-bonding; such structures are discussed more extensively in the 1D section.<sup>92,93,107,108</sup>

### 2.3. Molecular lattices

Molecular lattice structures are influenced by both molecule–substrate interfaces and the packing of the molecular backbones. The relative influence of these contributions can vary due to factors including interfacial bond strengths and sizes of the molecular backbones. Molecular interactions within lattices include van der Waals, dipole–dipole, and hydrogen-bonding interactions. van der Waals interactions between molecules in lattices contribute to stability. In alkanethiol–Au SAMs, this contribution increases with alkyl chain length, as each methylene ( $-CH_2-$ ) unit contributes approximately 1 kcal/mol.<sup>30</sup> Alkanethiolates on Au{111} tilt roughly  $30^\circ$  relative to the surface normal, to maintain nominally all-*trans* configurations that maximize van der Waals interactions.<sup>25,74</sup> As chain lengths increase in alkanethiols, the range of accessible backbone tilt angles is constrained due to steric effects.<sup>109</sup> Monolayers on other substrates have different tilt angles, again determined by the substrate lattice and maximizing intermolecular interactions.<sup>5,110</sup>

Chemical functional groups incorporated into the molecular backbone can influence molecular lattice structures. For instance, 3-mercapto-*N*-nonylpropionamide (1ATC9) is chemically similar to the more commonly used decanethiol, with an amide functional group replacing a methylene unit near the thiol headgroup. Two phases have been observed, one normal to the surface, the other tilted  $18^\circ$  relative to the surface normal.<sup>111</sup> The amide groups enable hydrogen bonding between molecules in the monolayer in the tilted conformation, increasing intermolecular interaction strength by  $\sim 6$  kcal/mol, and increasing the electronic polarizability of the monolayer.<sup>91,111,112</sup> Such interactions can cause phase segregation, creating monolayers with two distinct types of domains: 1ATC9 monolayers phase separate from *n*-alkanethiols of equivalent length based on their hydrogen-bonding networks.<sup>113</sup> Amide-bonding networks in SAMs have also been used for charge transport across Ag/SAM// $Ga_2O_3$ /EGaIn junctions.<sup>114</sup>

Even functional groups that introduce relatively strong interactions such as hydrogen bonding can disrupt monolayer formation if they interfere with molecular packing. The di-amide and tri-amide counterparts of the system described above, 3-mercapto-*N*-(*N'*-*n*-hexylacetamido)propionamide (2ATC9) and 3-mercapto-*N*-(*N'*-(*N'*'-*n*-propylacetamido)acetamido)propionamide, do not form ordered monolayers, at least in the outermost alkyl layers measured with the STM.<sup>113,115</sup>

Other chemical functional groups can be added within the molecular backbones to impact monolayer formation, including alkenes, alkynes, diacetylene, aryl groups, oligo(phenylene ethynylene), oligo(ethylene glycol), sulfones, and azobenzenes.<sup>14,15,25,116,117</sup> Functional groups can be used to create a wide variety of properties in monolayers, including switchable conductivity,<sup>118</sup> targeted capture of biological molecules,<sup>119</sup> or the ability to crosslink under an electron beam<sup>120</sup> or restructure under an ion beam<sup>121</sup> to act as a molecular resist.

Cage molecules such as adamantanes and carboranes are classes of SAM substituents in which the cage serves as a short, sterically bulky backbone.<sup>6,82,122,123</sup> Thiolated cage molecules thus have large molecular lattice constants relative to alkanethiols (~0.7 nm vs. 0.5 nm), and weaker intermolecular interactions,<sup>124</sup> meaning they are easily displaced from Au{111} surfaces by alkanethiols.<sup>6,123</sup> Adamantane cages can be engineered to orient normal or tilted relative to the surface, by thiolating at either a primary (2-adamantanethiol) or tertiary (1-adamantanethiol) carbon, making it possible to create or to eliminate tilt defects based on small changes in molecular structure.<sup>123</sup> Larger diamondoid structures also form monolayers with a variety of interesting structures and properties.<sup>6,125,126</sup>

As with alkanethiols, carboranethiols have been designed to have molecular dipoles that contribute to molecular lattice interactions;<sup>6,127</sup> carboranethiols with strong lateral dipole-dipole interactions dominate surface coverage when codeposited with carboranethiols that lack such interactions.<sup>127</sup> Dipole effects can also be important in noncovalently bound monolayers. For instance, styrene, under vacuum and low temperature, forms dipole-organized assemblies on Au{111}.<sup>104</sup>

## 2.4 Molecule-environment interfaces

Terminal functional groups determine the physical properties at environmental interfaces. Terminal group chemistries can vary widely, including methyl groups, amines, nitriles, carboxylic acids, sulfides, alcohols, ferrocenes, pyrroles, fullerenes, and biomolecules.<sup>1,119,128-137</sup>

Interface physical properties can be changed dramatically based on relatively straightforward chemical changes to terminal groups. The conventionally used methyl terminal group for alkanethiolates produces hydrophobic SAMs, whereas hydroxyl-terminated alkanethiols assemble into hydrophilic SAMs, even though the bulk of the backbone is hydrophobic. Similarly, SAMs can present large numbers of aligned dipoles at the interface, which can be reversed based on terminal substituents, for instance electron-rich amines vs. electron-poor nitriles.<sup>130</sup>

Specialized terminal groups create additional possibilities for monolayer function. Azobenzene terminal groups isomerize on exposure to UV (365 nm) and blue (450 nm) light, respectively.<sup>14,15,138</sup> Pyrrole-terminated SAMs polymerize upon plasma exposure, forming conductive and mechanically active polymers.<sup>134</sup> Hydroxyl-terminated SAMs have also been used to immobilize Au nanoparticles on surfaces.<sup>139</sup>

Simple functional groups displayed at SAM–environment interfaces can be used for further reactions to display more complex molecules on surfaces. Common functional groups incorporated into SAMs for reactions to create biological interfaces include carboxylic acids, amines, and azides.<sup>119,140–145</sup> Care is needed in further functionalization of SAMs as the reaction exothermicity of vigorous surface reactions can disrupt the assemblies and nanostructures previously formed.<sup>11,13,142,146</sup>

Carboxylic acids can be used in standard synthetic reactions (such as N-hydroxy-succinimide–ethylenediaminecarbodiimide, NHS-EDC, coupling) to create amide linkages – such reactions have been used to attach benzensulfonamide ligands for enzymes,<sup>147</sup> as well as for attachment of small-molecule neurotransmitters, their precursors, proteins, and other molecules.<sup>119,136,137</sup> Interactions with large molecules such as receptor proteins are in some cases more specific when ligands are distributed several nanometers apart on the surface; this is discussed further in the section on 0D assemblies. Amines, similarly, can be used for coupling reactions, which have been used to display functional groups including nitrophenyl phosphonates<sup>80,101</sup> and neurotransmitters<sup>148</sup> on surfaces, to interact with molecules in solution.

Azides displayed on surfaces can be used for a copper(I)-catalyzed azide–alkyne cycloaddition known as the ‘click’ reaction due to its high reaction efficiency.<sup>149</sup> This approach has been used, for instance, to attach peptides to surfaces to study cell adhesion.<sup>150,151</sup> This reaction has also been carried out using a copper AFM tip to create localized molecular patterns.<sup>152</sup>

### 3. One-dimensional assemblies

One-dimensional structures on surfaces can be templated by anisotropy in the surface, created by depositing anisotropic (inherently 1D) molecules, or can arise from interactions such as hydrogen bonding between molecules (Figure 3).<sup>52</sup> Once assemblies are formed, some types of molecules (such as those containing diacetylene functionalities) can polymerize to create covalently bound structures.<sup>8,153,154</sup> Linear structures may be aligned in a number of ways, including external electric or magnetic fields, or capillary interactions with a receding solvent.<sup>155</sup> One-dimensional assemblies have been used to create directionally conductive monolayers, for linear transport of nanoscale objects, and to induce macroscale motion by causing directional strain in a substrate.<sup>156–158</sup>

#### 3.1. Substrate surface reconstruction

Solid crystalline surfaces typically have unsatisfied bonds, in some cases leading the top layer of the surface to reconstruct to minimize surface energy, either on the pristine surface,<sup>41,159</sup> or as adsorbates bind.<sup>160</sup> For instance, pristine Si(100) surfaces prepared in ultrahigh vacuum ( $<10^{-10}$  torr) and thermally annealed, reconstruct to form Si dimers with  $\pi$ -bond character (the Si(100)– $2\times 1$  phase).<sup>41</sup> As noted above, such features can template assembly.

#### 3.2. Surface defects and electronic standing waves

Surface defects such as atomic step edges and vacancies cause perturbations in the local electronic density of states,<sup>105,161,162</sup> that modulate the binding of adsorbates and create linear arrays, as for benzene adsorbed to Cu{111} step edges.<sup>163</sup> Linear arrays of magnetic atoms<sup>105</sup> (such as Co on Pt{111})<sup>164</sup> have been of particular interest due to theoretical predictions of unique 1D magnetic properties.<sup>165,166</sup> Adsorbates can also perturb surface electronic structure and template the binding of further adsorbates,<sup>163,167</sup> as found for L-methionine on Ag{111}, which forms linear arrays<sup>168</sup> that can be used to template further adsorption of species such as Fe atoms.<sup>169</sup>

### 3.3 Anisotropic molecules

Adsorption of anisotropic molecules also leads to 1D surface structures. Both synthetic and natural linear molecules have been used for this purpose. Synthetic examples include bistable rotaxanes,<sup>170</sup> dumbbell-shaped molecules with controlled numbers of electron-accepting cyclobis(paraquat-*p*-phenylene) rings threaded on the shafts; each ring has a pair of available docking stations with which it associates via electron donor–acceptor interactions. Such molecules deposited on surfaces have been both characterized at the single-molecule level,<sup>171</sup> and used to do macroscale work (cantilever tip deflections up to 2  $\mu\text{m}$ ) based on electrochemically controlled motion of the rings between their two stable positions on the shaft.<sup>157,172</sup>

Natural 1D structures may also be studied on surfaces – DNA has been deposited on surfaces both in its natural linear state and as components of DNA origami structures with controlled morphology.<sup>173</sup> Linear origami structures have been used to perform assembly-line tasks, loading three different gold nanoparticles cargoes onto a DNA walker transiting the line (each step  $\sim 2$  h), in a programmable fashion.<sup>174,175</sup> Peptides forming regular secondary structures, such as  $\beta$  sheets, have been assembled on surfaces to illuminate the process of amyloid plaque formation.<sup>176</sup> Biologically important protein assemblies (such as muscular actin–myosin filaments) are also deposited on surfaces. Small (1–4  $\mu\text{m}$ ) metallized actin filaments have been used as nanoscale transporters on myosin-coated surfaces, with speeds of  $\sim 200$  nm/s (vs.  $\sim 4$   $\mu\text{m}$ /s for unmetallized actin), controlled by the addition of ATP.<sup>156</sup>

### 3.4 Noncovalent interactions

Noncovalent interactions between molecules, such as hydrogen-bonding or substrate-mediated interactions, are used to template 1D assembly. In addition to the hydrogen-bonded peptide structures mentioned above, organic molecules can form 1D arrays.<sup>52,105</sup> Typical structures include a rigid framework (often benzene, anthracene, or a porphyrin), and substituents that facilitate directional intermolecular interactions.<sup>4,177</sup>

For instance, dicarboxylic acids with long alkyl substituents (such as isophthalic and terephthalic acid derivatives) form linear arrays based on both hydrogen bonding between carboxylic acids and interdigitation of the long alkyl tails.<sup>4,7</sup> In this context, the interdigitated alkyl tails form 1D lamellar structures, with the carboxylic acids organizing at the periphery of each lamella. Lamellar structures can also be formed from other functionalized alkanes (including alcohols, amines, and bromides), or even long alkanes such as tricontane (30 carbons) based on van der Waals forces.<sup>178</sup> Tilt angles of the molecules relative to the lamellar axis vary based on interactions between the functional head groups.<sup>179</sup>

### 3.5 Polymerization

Polymerization of molecules self-assembled on surfaces can produce covalently bound 1D structures.<sup>8,153,154,180</sup> For example, diacetylene derivatives such as nonacos-10,12-diyonic acids have been assembled on HOPG, using long alkyl chains<sup>154</sup> or hydrogen-bonding functional groups such as isophthalic acids<sup>153</sup> to align the alkyne moieties. Polymerization is either initiated across the entire surface, using UV light,<sup>154</sup> or at a single point, using a STM probe tip.<sup>181</sup> Polymerization creates linear polydiacetylene chains that terminate at domain edges or defects, with HOMO-LUMO gaps that decrease with increasing chain length,<sup>154</sup> and conductivities that increase substantially (up to 1000 $\times$ ) with iodine doping.<sup>180</sup> Films of polymerized pentacos-10,12-diyonic ethanolamide exhibit source–drain modulation when a gate bias is applied, in contrast to less-ordered polymerized films,<sup>182</sup> suggesting the importance of aligning 1D features for applications in devices.



## 4. Zero-dimensional assemblies

Zero-dimensional molecular features consisting of individual molecules or small molecular clusters have been studied for their electronic, mechanical, magnetic, optical, biological, and chemical properties.<sup>21</sup> Studies at this level illuminate unique properties that otherwise are lost through averaging in ensemble measurements. Here, we select illustrative examples, classified based on molecular function (Figure 4).

Single-molecule electronic properties in particular have been extensively investigated with the goal of producing single-molecule devices performing the functions of macroscale circuit components.<sup>183,184</sup> Such studies began in 1974 with a theoretical proposal of a molecular rectifier by Aviram and Ratner,<sup>185</sup> and now encompass both theoretical and experimental work on molecular resistors, rectifiers, electronic and photochromic switches, and other devices.<sup>186–188</sup>

Just as decreasing the size of macroscale circuit components increases the importance of interface issues such as line edge roughness, the interface between a molecular device and its environment (including electrodes and surrounding molecules) is critical. Electrode–molecule coupling, determined by band alignment, contact bonding, and contact geometry, plays a critical role in electron transport properties. Thus, with proper control over electrode interfaces, electronic properties of contacts can be tuned.<sup>97,184,187,189</sup>

### 4.1 Characterization

Scanning probe microscopes are widely used for molecular electronic characterization, since they can both image target molecules in their environments and position one electrode (the scanning probe tip) with sub-nanometer precision in three dimensions.<sup>190–192</sup> In addition to interfaces with the substrate, nearby conductive molecules can influence the electronic properties of target molecules. To reduce the effects of such interactions, active molecules can be distributed in less conducting monolayer matrices.<sup>9,21</sup> One method for doing this is solution deposition of conductive molecules inserted into existing ordered alkanethiolate (or other) SAMs (Figure 4).<sup>9,10</sup> Target molecules have high probabilities of deposition at domain boundaries and other defects in SAMs, typically resulting in few-nm spacings between molecules, adequate for electrical isolation. This method was used by Weiss and co-workers to test the conductance switching mechanism of isolated oligo(phenylene ethynyl) (OPE) thiolate molecules inserted into self-assembled dodecanthiolate monolayers.<sup>9,19,193</sup>

Active molecules can also be co-deposited at low concentration *with* alkanethiolates, dispersing them within the alkanethiolate domains; however, high-temperature (~80 °C) annealing after deposition can cause the active molecules to phase segregate.<sup>194</sup>

Single molecules can be also suspended between contacts in break junctions.<sup>192,195,196</sup> In this configuration, one electrode is initially in contact with or in close proximity to the other, and is slowly drawn away to break contact. If bifunctional (for instance dithiolated) conductive molecules are present in the junction, quantized conductance decreases are observed as the number of molecules bridging the junction decreases. Junction lengths can be controlled to  $\pm 1$  Å, and the junction is typically broken and reformed repeatedly to test reproducibility. Alternatively, controlled junction lengths can be achieved in static conformations using techniques such as on-wire lithography.<sup>197</sup>

Further molecular measurements can be made using scanning tunneling spectroscopy.<sup>191</sup> Inelastic electron tunneling spectroscopy (IETS) is performed using STM by holding the tip stationary over a molecule (i.e., without varying the tip–sample separation or the lateral

position), and varying the voltage while monitoring the current at low temperature (4 K). This yields a current–voltage curve dependent on the vibrational spectrum of the molecule, providing both structural and electronic information about the single-molecule junction.<sup>198,199</sup> Comparable measurements have been made in break junctions.<sup>200,201</sup>

## 4.2 Molecular function

**4.2.1 Resistors**—Single-molecule conductance is sensitive to several factors, in addition to the chemical structures of molecules. These include the chemistry, geometry, and electronic properties of the contacts with the electrode (thiol, amine, etc.), as well as interactions with surrounding molecules.<sup>97,202–204</sup> Molecular energy levels (particularly the highest occupied molecular orbital, HOMO, and lowest unoccupied molecular orbital, LUMO) shift on binding to the electrodes. This shift determines the difference between molecular energy levels and the Fermi levels of the electrodes; alignment of either the HOMO or LUMO with the Fermi level typically increases conductivity.<sup>203,204</sup>

Conductance measurements based on repeated break-junction formation can generate histograms of values for thousands of Au–molecule–Au junctions, which are important due to variations in conductance with electrode geometry.<sup>205</sup> Conductance is often reported in relation to the quantum point contact value  $G_0 = 77.4 \mu\text{S}$ , which is the ideal conductance value for two metal electrodes bridged by a single atom of the same metal.<sup>202</sup> Conjugated molecules with extended  $\pi$  systems have higher conductances than unconjugated molecules such as alkanethiols.<sup>206</sup> Conductance also varies with the chemistry of the contacts, with reported conductance orders of  $\text{R–P} > \text{R–S} > \text{R–NH}_2 > \text{R–COOH}$  for saturated alkanes,<sup>207,208</sup> and differences between thiolates and selenolates.<sup>97</sup> Again, values and relative order depend on the specific backbones and electrodes, as band alignment effects dominate.<sup>209</sup>

**4.2.2 Rectifiers and diodes**—Certain molecules with two conjugated groups having donor–bridge–acceptor structures exhibit asymmetric conduction, or rectification.<sup>210</sup> Several factors contribute to rectification. One is the magnitude of the Schottky barrier at each interface, which depends on the mismatch between the molecular HOMO or LUMO and the substrate Fermi level.<sup>211,212</sup> Another is the placement of the donor–bridge–acceptor structure relative to the two electrodes. Asymmetric placement (often achieved using alkyl spacers with different lengths) increases rectification.<sup>121,213</sup> Rectification also occurs due to differences in energy levels between the donor and acceptor groups.<sup>213</sup> Distinguishing this contribution from the formation of a Schottky barrier requires the use of the same metal for both electrodes, first achieved by Metzger and coworkers.<sup>214</sup> Rectification ratios (ratio of conductances at positive and negative voltages of the same magnitude) of up to 3000 at  $\pm 1$  V have been measured in a cationic donor–bridge–acceptor dye (Fig. 4B).<sup>215</sup> Experimentally, the same challenges described above for resistors apply here; for instance, rectification depends on the structure of the junction between the electrodes. In addition, the rectification ratio has been observed to decrease with successive measurements, complicating quantification.

**4.2.3 Switches**—Molecular switches transition between two (or more) electronic, structural, or optical states in response to external stimuli. The behavior of most such molecules is initially characterized in solution. Surface-bound switching is of interest because it creates the possibility of using switch states in devices; however, surface attachment often impacts switching, meaning careful characterization is important.

Certain classes of molecules undergo switching between high and low conductance states. Oligo(phenylene ethynylene)s are widely studied examples, in which switching occurs due

to hybridization changes at the metal–molecule contact.<sup>16,19</sup> As with the molecules discussed above, switching behavior depends on the local environment. For instance, placing OPE molecules in well-ordered alkanethiol SAM matrices increases stability and reduces stochastic switching frequency. Hydrogen-bonding interactions with appropriately designed amide-containing alkanethiol SAMs have been used to stabilize one or both switch states.<sup>18,216</sup>

Photochromic molecules switch between conformational states upon exposure to light of characteristic wavelengths, with switching behavior that is often different on surfaces vs. in solution. For instance, azobenzene molecules, containing two benzene rings linked through an N=N double bond, undergo photoisomerization from a lower-energy *trans* conformation to a higher-energy *cis* conformation when irradiated at ~365 nm.<sup>217</sup> Isomerization on surfaces introduces additional considerations. If molecules lie flat on bare metal surfaces, isomerization is typically quenched due to electronic coupling with the surface.<sup>217,218</sup> If molecules are elevated off the surface on bulky legs to decouple them from the substrate, switching is again observed;<sup>218</sup> however, the photon absorption cross-section is reduced relative to that in solution,<sup>219</sup> and the reaction can proceed via a different mechanism.<sup>220</sup> Switching can also be achieved by depositing the molecules at defects in background SAM matrices, linked to the surface through tethers long enough to place the azo functionality protruding beyond the matrix.<sup>15</sup> In this case, the structure of the tether plays a key role in mediating switching.<sup>209,218,221</sup>

Placing functional molecules on surfaces also opens new possibilities for controlling switching. For instance, azobenzene switching on surfaces can be initiated using electric fields or tunneling electrons from a STM probe tip.<sup>209</sup>

Mechanically interlocked molecules such as catenanes and rotaxanes operate based on the motion of two or more noncovalently linked molecules relative to each other.<sup>222–225</sup> Rotaxanes are comprised of dumbbell-shaped molecules with a ring-shaped molecule threaded on the shaft. The ring can move between two stations on the shaft based on the oxidation state of the preferred tetrathiafulvalene (TTF) station. Tethering these molecules to solid surfaces enables them to perform work,<sup>157</sup> but also raises the possibility that interactions with the surface or neighboring molecules may affect their function.

The motion of individual rings can be tracked using electrochemical STM (with solution covering the surface), as the potential is raised and lowered (from ~0.1 to ~0.5 V), reversibly changing the oxidation state of the TTF station. Since the shafts are much less conductive than the rings, only the rings are visible in STM images. Observing the motions of ~100 rings as the potential is cycled reveals a distribution of ring displacements around the ~3 nm distance between stations of the fully extended molecule, with an average displacement of ~2 nm.<sup>171</sup> This suggests that the shaft binds to the surface without the ends fully extended. Direct measurements such as those described inform strategies for optimizing molecular function for devices, such as development of rotaxane switches with more rigid shafts. Rigid shafts would have the further advantage of being able to transmit greater force in assembled, cooperative devices.<sup>157,158</sup>

**4.2.4 Single-molecule reactions**—Isolating individual molecules or pairs of molecules on surfaces as 0D structures enables chemical reactions to be initiated and monitored at the single-molecule level. Again, STM is a useful tool, since electronic excitation can trigger chemical reactions, which can then be observed with the microscope; many STM measurements are performed at low temperature (4 K) under ultrahigh vacuum conditions (pressures <10<sup>-10</sup> torr), both reducing the likelihood of unwanted side reactions with gas-phase molecules, and slowing reaction kinetics.<sup>226</sup>

Such single-molecule chemistry was pioneered by Ho,<sup>227</sup> and Meyer and Rieder.<sup>228</sup> Ho and coworkers performed single-molecule dissociation of pyridine and benzene molecules on Cu(001).<sup>227</sup> Meyer, Rieder, and coworkers induced Ullmann coupling (formation of biphenyl from two iodobenzene molecules) on Cu{111}.<sup>228</sup> Weiss and coworkers later extended single-molecule reaction studies, inducing Ullman coupling with a scanning tunneling microscope and differentiating reactive intermediates from products based on IETS measurements.<sup>229</sup> Reaction mechanisms for catalytic chemistry on metal surfaces are technologically important, and often difficult to monitor using standard characterization techniques under reaction conditions.

In addition to observing important and normally short-lived reaction intermediates, 0D molecular assemblies on surfaces can be used to control reaction pathways to select for paths that would be unfavorable in solution. Pairs of thiolated anthracene phenylene ethynylene derivatives deposited at defects in alkanethiolate SAMs are confined in head-to-head arrangements.<sup>230</sup> When photoexcited, the molecules dimerize via cycloaddition, since they cannot access the head-to-tail conformation that would otherwise be sterically favored in solution.

**4.2.5 Biological applications of 0D assembly**—Isolating individual biomolecules on surfaces provides unique opportunities for understanding their structure and function,<sup>21,231–233</sup> although many systems benefit from careful selection of passivating monolayers to control interactions between the target molecules and the substrates.<sup>1</sup> Proteins are relatively large (~4 nm diameter for a 50 kD globular protein<sup>234</sup>) and can interact with other nearby proteins on surfaces, meaning that if proteins are targeted to surfaces by ligands, it is useful to have the ligands distributed several nanometers apart on surfaces. This is possible using the defect-based insertion strategy discussed previously.<sup>137,235</sup> For instance, 5-hydroxytryptophan (5-HTP), a serotonin precursor, has been covalently bound to tethers via its additional carboxyl group. The use of insertion-directed self-assembly distributes 5-HTP at defects in SAM matrices, effectively spacing these molecules far apart. The use of the 5-HTP precursor, instead of the neurotransmitter serotonin (5-hydroxytryptamine) itself, leaves all epitopes of serotonin accessible for molecular recognition. These surfaces have been used to capture native serotonin receptor proteins.<sup>119,148</sup> Substrates capable of biomolecule-specific recognition can ultimately be used in tandem with other methods, such as surface mass spectrometry, to identify new target molecules.<sup>145</sup>

## 5. Molecular patterning and its applications

In the previous sections, we have described how molecular interactions of alkanethiols within SAMs and with the surrounding environment can be controlled and characterized to provide structural and functional information with sub-nanometer resolution. Integrating such functions into electronic and biosensing devices requires registry with macroscale features, often created by larger scale molecular patterning. Molecular patterning has been carried out on a variety of solid surfaces (including Au, Ag, Cu, Ge, Pd, and SiO<sub>2</sub>), utilizing an array of techniques in surface chemistry to generate patterns ranging in scale from microns to nanometers.<sup>44,47,49,236–240</sup> Terminal functional groups displayed at interfaces define both physical and chemical surface properties, making it possible to tailor surfaces down to the nanoscale through chemical patterning.<sup>14,15,241–247</sup> In this section, we briefly discuss molecular patterning of SAMs through soft lithography, scanning probe lithography, and related techniques. Detailed descriptions of these techniques have been provided elsewhere and in previous reviews.<sup>1,11,25,248–253</sup>

## 5.1 Patterning strategies

**5.1.1 Soft lithography**—In soft lithography, a pliable elastomeric stamp is molded from polydimethylsiloxane (PDMS) or another polymeric material; molecular inks are then applied to stamps, which are used to transfer inks to surfaces, reproducing the stamp features.<sup>254</sup> Stamps are typically produced by casting liquid PDMS onto master molds with predefined features fabricated by photolithography or EBL. Features in masters are negatively replicated in PDMS stamps. For example, trenches and protruding features on the master molds will create protruding and depressed features on PDMS stamps, respectively.

Although a variety of molecular inks are currently available, alkanethiols are the original (and still the most commonly used) inks for conventional soft lithography.<sup>254</sup> The soft PDMS stamp conforms to the surface topography of substrates, making it possible to pattern curved substrates.<sup>255</sup>

Molecular ink features can be used in several ways. Inked patterns act as chemical etch resists, protecting patterned areas while material in the exposed areas is removed.<sup>256,257</sup> As a result, stamp features are transferred into the underlying solid substrates. Unpatterned areas can also be backfilled, to self-assemble different molecules to create surfaces displaying chemically distinct functional groups in patterned vs. unpatterned areas. Such surfaces have been investigated in the context of preventing biofouling<sup>258–260</sup> and guiding cell growth.<sup>261,262</sup>

Two key factors relating to inks limit the fidelity of feature reproduction in soft lithography. Alkanethiol inks can diffuse laterally on the surfaces of substrates beyond the contact areas (surface diffusion) during printing, creating halos around patterned features.<sup>235</sup> Additionally, low molecular weight inks are volatile, enabling ink vapor deposition in noncontacted areas.<sup>263</sup> Both phenomena decrease pattern fidelity, becoming more important as feature sizes are reduced to the nanoscale. Several modifications to soft lithography have been developed to address these challenges.<sup>235,244,254,264,265</sup>

**5.1.2 High-molecular-weight inks**—Using higher molecular weight inks lowers ink vapor pressure, reducing vapor deposition to noncontacted areas during ink transfer.<sup>263,266</sup> High-molecular-weight inks also minimize lateral diffusion around patterned features. For instance, Delamarche *et al.* demonstrated that by controlling both ink concentration and stamp-substrate contact time, microcontact printing of eicosanethiol (a 20-carbon alkanethiol) can be used to create features ~80 nm in size.<sup>263</sup> Even smaller feature sizes (~40 nm) were achieved using dendrimeric polymers, which are more massive than commercially available alkanethiols.<sup>267</sup> Although high-molecular-weight inks minimize lateral diffusion and vapor deposition, their sizes can cause inks to precipitate on stamp surfaces prior to contact, causing post-printing patterning problems on substrates.<sup>268</sup> In addition, polymeric inks do not provide robust etch resist properties for device fabrication.<sup>269</sup>

**5.1.3 Microcontact displacement printing ( $\mu$ DP)**—Another method for retaining line edge sharpness by preventing lateral diffusion of alkanethiol inks is referred to as microcontact displacement printing.<sup>142,265,270</sup> Here, labile adamantaneethiols are first self-assembled on substrates. Because adamantaneethiols have weak intermolecular interactions, lower molecule–substrate bond densities, and mismatched lattices relative to the displacing molecules, they are readily displaced by alkanethiol inks in the stamped areas. Adamantaneethiol molecules remaining in the unpatterned regions around patterned features prevent ink molecules from diffusing outside the contact areas, improving line-edge roughness.<sup>265</sup> An important consideration in this method is that the molecular ink must form

a sufficiently robust monolayer to displace the existing weakly bound adamantanethiol SAM.

**5.1.4 Microcontact insertion printing ( $\mu$ CIP)**—If surfaces are instead passivated with more strongly bound alkanethiol SAMs prior to patterning, ink molecules are inserted at defects in the existing SAMs (as opposed to displacement).<sup>271,272</sup> This produces dilute patterns of ink molecules in the stamped areas. For work with biomolecules, this capability is particularly useful. If small-molecule probe molecules are distributed across surfaces at defects, relatively large target proteins and antibodies can be captured specifically based on function.<sup>119,137,140,141,148,273,274</sup> In contrast, full monolayers of small-molecule targets result in non-specific binding, because of the prevalence of exposed interacting functional groups.<sup>137,141,275</sup>

**5.1.5 Reactive spreading lithography**—If ink vapor formation is restricted, lateral diffusion of inks can be used to advantage to create nanoscale gaps between patterned areas by carefully controlling both ink concentration and stamp-substrate contact time. Xia *et al.* performed microcontact printing under water, regulating lateral ink diffusion to create alkanethiol SAM features separated by  $\sim$ 100 nm gaps.<sup>276</sup> Because stamps and substrates were immersed in water and a relatively high-molecular-weight, water-insoluble ink was used, ink vapor was not formed. Controlled lateral spreading has also been exploited in a technique called edge spreading lithography, discussed below.<sup>277</sup>

**5.1.6 Catalytic microcontact printing**—In contrast to the techniques discussed above, catalytic microcontact printing ( $C\mu$ CP) patterns substrates without requiring ink transfer, avoiding altogether problems associated with lateral and vapor diffusion. In this technique, polymeric stamp surfaces are functionalized or inked with chemical species that catalyze reactions or react with functional groups on substrates in stamped areas.<sup>278</sup> A notable feature of  $C\mu$ CP is the interfacial reaction that takes place between the chemically functionalized surfaces of polymeric stamps and the reactive surfaces of SAM-modified substrates. The mechanism of interfacial reactions has been widely discussed, since tethering both reaction partners to solid surfaces would be expected to hinder their reaction.<sup>279,280</sup>

Patterning with  $C\mu$ CP has produced feature sizes as small as  $\sim$ 20 nm and found diverse applications in surface chemistry, biology, and catalysis.<sup>144,281–283</sup> Key concerns for  $C\mu$ CP include optimizing chemical conjugation for the polymeric stamps and eliminating competing conjugating pathways that reduce reaction yields.<sup>284</sup> Extension to smaller feature sizes ( $<$ 20 nm) would enable single-molecule biological studies.

**5.1.7 Chemical lift-off lithography**—Chemical lift-off lithography (CLL)<sup>58</sup> extends the concept of  $C\mu$ CP by allowing reactions to take place between stamp surfaces and substrate-bound SAMs, which is followed by lift-off of reacted molecules from monolayers as the stamp is removed. In CLL, PDMS stamps with molded relief patterns are activated by oxygen plasma treatment and brought into conformal contact with SAM-modified Au substrates. The activated patterns react with certain classes of chemical functional groups on the exposed surfaces (*e.g.*, alcohols but not unmodified alkanes). Contact-induced reactions form covalent bonds, allowing reacted molecules to be lifted off surfaces in areas where the stamps make contact.<sup>58</sup> Exposed gold areas can either be chemically etched or backfilled with other alkanethiols to create multicomponent patterned SAMs. For example, biotin-terminated alkanethiols were self-assembled on post-lift-off hydroxyl tri(ethylene glycol) SAM-modified Au substrates, to create small-molecule patterned substrates for biorecognition. Patterning by CLL can produce sharp 40-nm gaps with a single patterning

step using nanopatterned masters;<sup>58</sup> alternatively, micropatterned masters can be shifted in registry through multiple lift-off steps to produce features narrower than 50 nm.

Investigation of post-lift-off PDMS stamps by X-ray photoelectron spectroscopy indicated that Au was removed from the underlying substrates, suggesting that the stamp-SAM interactions are at least as strong as the Au–Au bonds at the substrate surface. Thus, CLL serves as a potential route to investigate the widely discussed nature of SAM-substrate interactions.

## 5.2 Scanning probe lithography

As described in previous sections, scanning probe microscopy can be used to characterize and provide structures and function of alkanethiol SAMs on solid substrates with Ångström resolution. In this section, we discuss the use of scanning probe microscopy in lithography to achieve high-resolution molecular nanoscale patterning, including AFM-based techniques such as dip-pen nanolithography (DPN), nanografting, nanoshaving, and STM-based techniques.

### 5.2.1 Techniques based on atomic force microscopy: Dip-pen nanolithography and nanografting

—Dip-pen nanolithography, developed and commercialized by Mirkin and coworkers, transfers molecular ink from an AFM tip to substrates via a water meniscus.<sup>251</sup> Because ink transfer is mediated by the meniscus, feature size and resolution are controlled not only by the probe tip sharpness (the probe tip radius of curvature is typically ~10 nm), but also by tip–surface contact duration, ink diffusion dynamics, chemical structures of molecular inks, temperature, and relative humidity.<sup>285–287</sup> Thiols, proteins, nucleotides, DNA, and polymers have all been used as molecular inks for DPN.<sup>251,288–296</sup> Relative to microcontact printing, DPN typically produces smaller features but at slower speeds since it is a serial process. However, patterning speeds are increased by utilizing multiple tips simultaneously.<sup>275,297–300</sup>

While DPN uses an AFM tip to add molecules to substrates, molecules in SAMs can also be removed by dragging the tips through SAMs with scanning forces higher than those used for imaging, a process referred to as nanoshaving.<sup>301,302</sup> Performing this process with the surface immersed in a solution of different SAM-forming molecule is called nanografting, and allows the exposed areas to be backfilled by other molecules, creating multi-component surfaces.<sup>302</sup> These techniques retain the properties of high spatial resolution and can be performed under many different chemical environments.<sup>303</sup> They have been widely used for fabricating molecular patterns with sub-100-nm resolution.<sup>301,304–307</sup> Nanografting has been used to regulate and to study reaction mechanisms,<sup>308</sup> and to fabricate multicomponent nanostructures for molecular electronic and biological applications.<sup>274,301,309–311</sup>

Similar to DPN, the main limitations of nanoshaving and nanografting are relatively slow patterning speeds and small patterning areas. However, in addition to creating arbitrary 2D patterns, 3D nanostructures can also be fabricated through simple chemical reactions on features created by nanografting.<sup>312</sup>

### 5.2.2 Techniques based on scanning tunneling microscopy

—Similar to AFM-based patterning techniques, STM tips can also be used to create high-resolution (sub-20 nm) patterns by applying high biases (3–4 V, in contrast to typical imaging voltages of magnitude ~1 V) between the STM probe tip and conducting or semiconducting samples, causing desorption of molecules from surfaces.<sup>313,314</sup> If desorption is performed under a liquid, exposed areas can be backfilled with other molecules, a process known as STM-replacement lithography (STM-RL).<sup>315,316</sup> Although this technique produces precise features, patterns are formed slowly and only over small areas, even relative to AFM-based

techniques. Additionally, high applied biases can chemically modify the STM probe tip itself, decreasing feature precision.<sup>11</sup>

### 5.3 Other techniques

In addition to conventional soft-lithography and scanning probe lithography techniques described above, other strategies have also produced high-quality molecular-scale patterns. In this section, we will discuss two examples of unconventional patterning strategies: edge spreading lithography and molecular rulers.

**5.3.1 Edge spreading lithography**—Lateral diffusion of alkanethiol inks can be controlled to fabricate patterns on Au substrates.<sup>276</sup> Edge spreading lithography (ESL) leverages diffusion in a multi-step process to create narrow features *only* in areas to which the ink diffuses, rather than in both stamped and diffusion-coated areas. Elastomeric stamps first transfer alkanethiols to substrates with existing template features. The ink diffuses along the template features to the surface, creating narrow molecular features around their edges.<sup>277,317</sup> Subsequent removal of the template leaves narrow molecular features on substrates. The template features can either be patterned through conventional lithography or by techniques such as colloidal lithography; the use of conventional lithography enables patterning over large areas, while colloidal lithography enables creation of relatively small features.<sup>317</sup>

Multiple rounds of ESL can be performed on the same surface with different molecules, creating concentric patterns around the preformed features.<sup>318</sup> This procedure provides precise 2D control of chemical patterns on surfaces for applications in metal nanostructure fabrication and biology.<sup>318,319</sup>

**5.3.2 Molecular ruler lithography**—Molecular ruler lithography combines a top-down patterning approach (EBL) with a bottom-up approach (SAM formation) to fabricate high-resolution nanostructures.<sup>320</sup> Parent features are first fabricated through EBL or photolithography. Subsequently, multiple SAMs with well-defined thicknesses are deposited on the parent features through electrostatic interactions, by alternating layers of end-functionalized  $\alpha,\omega$ -mercaptoalkanoic acid with layers of a polycation. This process creates small, precisely controlled gaps (4–100 nm) between two parent features. Importantly, the chemistry of the parent features, substrate, and SAM constituents must be chosen such that the SAMs wet only the parent features and not the substrate. Finally, daughter features are created through controlled deposition of metals across the entire surface; removing the SAM layers reveals the original parent features, as well as daughter features formed in the gaps. The lengths of the molecules and the numbers of alternating layers used to create the multilayer resists control feature thickness, acting as a ruler to vary both the spacing between the parent and daughter features and the daughter feature sizes.<sup>320–334</sup> This process expands chemical patterning control of molecules from 2D to 3D.

## 6. Perspectives

Molecular monolayers represent one of the limits of nanostructured materials, and, in some cases, enable control of structure and environment down to the single-molecule level. In 2D monolayers, the molecular lattice structures and physical properties can be tuned based on substrate structures, and the steric and chemical functionalities of the molecules making up the monolayers. Combining monolayer strategies with top-down patterning enables 2D monolayer structures to be created with features with below 100 nm to the wafer scale.<sup>11</sup> The self- and directed-assembly strategies described above enable control down to the sub-nanometer scale.



To date, the properties of 2D monolayers have been explored extensively; however, restricting additional dimensions can provide even greater control over function and provide insight into molecular processes. For instance, 1D structures can direct coupling between atoms and molecules or enable motion of nanoscale objects across surfaces, while 0D structures allow the course of individual molecular reactions to be controlled and monitored.

Studying molecular structures and processes at the sub-nanometer scale in real space makes it uniquely possible to understand how nanoscale properties change based on interactions with the environment, particularly defects and neighboring molecules. Since interfaces, defects, and heterogeneous structures are critical in applications from device performance to biological function, characterization tools that provide additional information about interfaces will open new fields of study and new means of control.

## Acknowledgments

We thank the Department of Energy (Grants #DE-FG02-08ER46546 and #DE-FG02-07ER15877), the National Science Foundation (Grants #CHE-1013042 and #CHE-1124984), and the Kavli Foundation for support of the work described here. S.A.C. acknowledges support from an NIH Postdoctoral Fellowship (7F32GM0892202).

## References

1. Love JC, Estroff LA, Kriebel JK, Nuzzo RG, Whitesides GM. *Chem Rev.* 2005; 105:1103–1169. [PubMed: 15826011]
2. Nuzzo RG, Zegarski BR, Dubois LH. *J Am Chem Soc.* 1987; 109:733–740.
3. Dubois LH, Nuzzo RG. *Annu Rev Phys Chem.* 1992; 43:437–463.
4. De Feyter S, De Schryver FC. *Chem Soc Rev.* 2003; 32:139–150. [PubMed: 12792937]
5. Poirier GE. *Chem Rev.* 1997; 97:1117–1127. [PubMed: 11851444]
6. Hohman JN, Claridge SA, Kim M, Weiss PS. *Mat Sci Eng R.* 2010; 70:188–208.
7. De Feyter S, Gesquiere A, Abdel-Mottaleb MM, Grim PCM, De Schryver FC, Meiners C, Sieffert M, Valiyaveetil S, Mullen K. *Acc Chem Res.* 2000; 33:520–531. [PubMed: 10955982]
8. Okawa Y, Aono M. *Nature.* 2001; 409:683–684. [PubMed: 11217849]
9. Bumm LA, Arnold JJ, Cygan MT, Dunbar TD, Burgin TP, Jones L, Allara DL, Tour JM, Weiss PS. *Science.* 1996; 271:1705–1707.
10. Cygan MT, Dunbar TD, Arnold JJ, Bumm LA, Shedlock NF, Burgin TP, Jones L, Allara DL, Tour JM, Weiss PS. *J Am Chem Soc.* 1998; 120:2721–2732.
11. Saavedra HM, Mullen TJ, Zhang PP, Dewey DC, Claridge SA, Weiss PS. *Rep Prog Phys.* 2010; 73:036501.
12. Weiss PS. *Acc Chem Res.* 2008; 41:1772–1781. [PubMed: 18847229]
13. Bumm LA, Arnold JJ, Charles LF, Dunbar TD, Allara DL, Weiss PS. *J Am Chem Soc.* 1999; 121:8017–8021.
14. Zheng YB, Payton JL, Chung CH, Liu R, Cheunkar S, Pathem BK, Yang Y, Jensen L, Weiss PS. *Nano Lett.* 2011; 11:3447–3452. [PubMed: 21749070]
15. Kumar AS, Ye T, Takami T, Yu BC, Flatt AK, Tour JM, Weiss PS. *Nano Lett.* 2008; 8:1644–1648. [PubMed: 18444688]
16. Moore AM, Dameron AA, Mantooth BA, Smith RK, Fuchs DJ, Ciszek JW, Maya F, Yao Y, Tour JM, Weiss PS. *J Am Chem Soc.* 2006; 128:1959–1967. [PubMed: 16464097]
17. Lewis PA, Inman CE, Yao Y, Tour JM, Hutchison JE, Weiss PS. *J Am Chem Soc.* 2004; 126:12214–12215. [PubMed: 15453724]
18. Lewis PA, Inman CE, Maya F, Tour JM, Hutchison JE, Weiss PS. *J Am Chem Soc.* 2005; 127:17421–17426. [PubMed: 16332092]
19. Donhauser ZJ, Mantooth BA, Kelly KF, Bumm LA, Monnell JD, Stapleton JJ, Price DW Jr, Rawlett AM, Allara DL, Tour JM, Weiss PS. *Science.* 2001; 292:2303–2307. [PubMed: 11423655]

20. Saavedra HM, Barbu CM, Dameron AA, Mullen TJ, Crespi VH, Weiss PS. *J Am Chem Soc.* 2007; 129:10741–10746. [PubMed: 17685611]
21. Claridge SA, Schwartz JJ, Weiss PS. *ACS Nano.* 2011; 5:693–729. [PubMed: 21338175]
22. Bigelow WC, Pickett DL, Zisman WA. *Journal of Colloid Science.* 1946:1.
23. Sagiv J. *J Am Chem Soc.* 1980:102.
24. Nuzzo RG, Allara DL. *J Am Chem Soc.* 1983; 105:4481–4483.
25. Smith RK, Lewis PA, Weiss PS. *Prog Surf Sci.* 2004; 75:1–68.
26. Bent SF. *ACS Nano.* 2007; 1:10–12. [PubMed: 19203125]
27. Laibinis PE, Whitesides GM, Allara DL, Tao YT, Parikh AN, Nuzzo RG. *J Am Chem Soc.* 1991; 113:7152–7167.
28. Ulman A. *Chem Rev.* 1996; 96:1533–1554. [PubMed: 11848802]
29. Shaporenko A, Ulman A, Terfort A, Zharnikov M. *J Phys Chem B.* 2005; 109:3898–3906. [PubMed: 16851442]
30. Vericat C, Vela ME, Benitez G, Carro P, Salvarezza RC. *Chem Soc Rev.* 2010; 39:1805–1834. [PubMed: 20419220]
31. Azzaroni O, Vela ME, Fonticelli M, Benítez G, Carro P, Blum B, Salvarezza RC. *J Phys Chem B.* 2003; 107:13446–13454.
32. Love JC, Wolfe DB, Haasch R, Chabynyc ML, Paul KE, Whitesides GM, Nuzzo RG. *J Am Chem Soc.* 2003; 125:2597–2609. [PubMed: 12603148]
33. Florida Addato, MaA; Rubert, AA.; Benítez, GA.; Fonticelli, MH.; Carrasco, J.; Carro, P.; Salvarezza, RC. *J Phys Chem C.* 2011; 115:17788–17798.
34. Zangmeister CD, Picraux LB, van Zee RD, Yao Y, Tour JM. *Chem Phys Lett.* 2007; 442:390–393.
35. Bengio S, Fonticelli M, Benitez G, Creus AH, Carro P, Ascolani H, Zampieri G, Blum B, Salvarezza RC. *J Phys Chem B.* 2005; 109:23450–23460. [PubMed: 16375318]
36. Mani G, Johnson DM, Marton D, Dougherty VL, Feldman MD, Patel D, Ayon AA, Agrawal CM. *Langmuir.* 2008; 24:6774–6784. [PubMed: 18512878]
37. Nakamura T, Miyamae T, Nakai I, Kondoh H, Kawamoto T, Kobayashi N, Yoshimura YSD, Ohta T, Nozoye H, Matsumoto M. *Langmuir.* 2005; 21:3344–3353. [PubMed: 15807573]
38. Rampi MA, Schueller OJA, Whitesides GM. *Appl Phys Lett.* 1998; 72:1781–1783.
39. Chiechi RC, Weiss EA, Dickey MD, Whitesides GM. *Angew Chem-Int Edit.* 2008; 47:142–144.
40. Hohman JN, Kim M, Wadsworth GA, Bednar HR, Jiang J, LeThai MA, Weiss PS. *Nano Lett.* 2011; 11:5104–5110. [PubMed: 22023557]
41. Buriak JM. *Chem Rev.* 2002; 102:1271–1308. [PubMed: 11996538]
42. Bent SF. *Surf Sci.* 2002; 500:879–903.
43. Kachian JS, Wong KT, Bent SF. *Acc Chem Res.* 2010; 43:346–355. [PubMed: 20041705]
44. Hohman JN, Kim M, Bednar HR, Lawrence JA, McClanahan PD, Weiss PS. *Chem Sci.* 2011; 2:1334–1343.
45. McGuinness CL, Shaporenko A, Mars CK, Uppili S, Zharnikov M, Allara DL. *J Am Chem Soc.* 2006; 128:5231–5243. [PubMed: 16608359]
46. Lim H, Carraro C, Maboudian R, Pruessner MW, Ghodssi R. *Langmuir.* 2004; 20:743–747. [PubMed: 15773100]
47. Wasserman SR, Tao YT, Whitesides GM. *Langmuir.* 1989; 5:1074–1087.
48. Schreiber F. *Prog Surf Sci.* 2000; 65:151–256.
49. Maury P, Peter M, Mahalingam V, Reinhoudt DN, Huskens J. *Adv Funct Mater.* 2005; 15:451–457.
50. Ito T, Forman SM, Cao C, Li F, Eddy CR, Mastro MA Jr, Holm RT, Henry RL, Hohn KL, Edgar JH. *Langmuir.* 2008; 24:6630–6635. [PubMed: 18522438]
51. Noble-Luginbuhl AR, Nuzzo RG. *Langmuir.* 2001; 17:3937–3944.
52. Elemans JAAW, Lei S, De Feyter S. *Angew Chem-Int Edit.* 2009; 48:7298–7332.
53. De Feyter S, De Schryver FC. *J Phys Chem B.* 2005; 109:4290–4302. [PubMed: 16851494]
54. Xu L, Miao X, Ying X, Deng W. *J Phys Chem C.* 2012; 116:1061–1069.

55. Xue Y, Zimmt MB. *J Am Chem Soc.* 2012; 134:4513–4516. [PubMed: 22369569]
56. Somorjai, GA.; Li, Y. *Introduction to Surface Chemistry and Catalysis.* John Wiley and Sons, Inc; Hoboken, New Jersey: 2010.
57. Duke CB. *Chem Rev.* 1996; 96:1237–1259. [PubMed: 11848788]
58. Liao WS, Cheunkar S, Cao HH, Bednar HR, Andrews AM, Weiss PS. *Science.* 2012 in press.
59. Tierney HL, Han JW, Jewell AD, Iski EV, Baber AE, Sholl DS, Sykes ECH. *J Phys Chem C.* 2011; 115:897–901.
60. Bellisario DO, Jewell AD, Tierney HL, Baber AE, Sykes ECH. *J Phys Chem C.* 2010; 114:14583–14589.
61. Tierney HL, Baber AE, Sykes ECH, Akimov A, Kolomeisky AB. *J Phys Chem C.* 2009; 113:10913–10920.
62. Jensen SC, Baber AE, Tierney HL, Sykes EC. *ACS Nano.* 2007; 1:22–29. [PubMed: 19203127]
63. Han P, Mantooth BA, Sykes ECH, Donhauser ZJ, Weiss PS. *J Am Chem Soc.* 2004; 126:10787–10788. [PubMed: 15327339]
64. Yu M, Bovet N, Satterley C, Bengió S, Lovelock K, Milligan P, Jones R, Woodruff D, Dhanak V. *Phys Rev Lett.* 2006; 97:166102. [PubMed: 17155415]
65. Stranick SJ, Parikh AN, Allara DL, Weiss PS. *J Phys Chem.* 1994; 98:11136–11142.
66. Hakkinen H. *Nat Chem.* 2012; 4:443–455. [PubMed: 22614378]
67. Maksymovych P, Voznyy O, Dougherty DB, Sorescu DC, Yates JT. *Prog Surf Sci.* 2010; 85:206–240.
68. Cossaro A, Mazzarello R, Rousseau R, Casalis L, Verdini A, Kohlmeyer A, Floreano L, Scandolo S, Morgante A, Klein ML, Scoles G. *Science.* 2008; 321:943–946. [PubMed: 18703737]
69. Chaudhuri A, Lerotholi TJ, Jackson DC, Woodruff DP, Dhanak VR. *Surf Sci.* 2010; 604:227–234.
70. Mazzarello R, Cossaro A, Verdini A, Rousseau R, Casalis L, Danisman M, Floreano L, Scandolo S, Morgante A, Scoles G. *Phys Rev Lett.* 2007; 98:016102. [PubMed: 17358489]
71. Otálvaro D, Veening T, Brocks G. *J Phys Chem C.* 2012; 116:7826–7837.
72. Iski EV, El-Kouedi M, Calderon C, Wang F, Bellisario DO, Ye T, Sykes ECH. *Electrochim Acta.* 2011; 56:1652–1661.
73. Monnell JD, Stapleton JJ, Jackiw JJ, Dunbar T, Reinerth WA, Dirk SM, Tour JM, Allara DL, Weiss PS. *J Phys Chem B.* 2004; 108:9834–9841.
74. Han P, Kurland AR, Giordano AN, Nanayakkara SU, Blake MM, Pochas CM, Weiss PS. *ACS Nano.* 2009; 3:3115–3121. [PubMed: 19772297]
75. Murphy KL, Tysoe WT, Bennett DW. *Langmuir.* 2004; 20:1732–1738.
76. Lio A, Charych DH, Salmeron M. *J Phys Chem B.* 1997; 101:3800–3805.
77. Allara DL, Parikh AN, Rondelez F. *Langmuir.* 1995; 11:2357–2360.
78. Bourgeat-Lami E. *J Nanosci Nanotech.* 2002; 2:1–24.
79. Jewell A, Tierney H, Sykes E. *Phys Rev B.* 2010; 82:205401.
80. Gouzman I, Dubey M, Carolus MD, Schwartz J, Bernasek SL. *Surf Sci.* 2006; 600:773–781.
81. Jewell AD, Kyran SJ, Rabinovich D, Sykes EC. *Chem Eur J.* 2012; 18:7169–7178. [PubMed: 22532331]
82. Hohman JN, Kim M, Schupbach B, Kind M, Thomas JC, Terfort A, Weiss PS. *J Am Chem Soc.* 2011; 133:19422–19431. [PubMed: 21861500]
83. Huang FK, Horton RC, Myles DC, Garrell RL. *Langmuir.* 1998; 14:4802–4808.
84. Taylor CE, Schwartz DK. *Langmuir.* 2003; 19:2665–2672.
85. Lim MS, Feng K, Chen XX, Wu N, Raman A, Nightingale J, Gawalt ES, Korakakis D, Hornak LA, Timperman AT. *Langmuir.* 2007; 23:2444–2452. [PubMed: 17261036]
86. Li J, Li X, Ni X, Wang X, Li H, Leong KW. *Biomater.* 2006; 27:4132–4140.
87. Uemura S, Tanoue R, Yilmaz N, Ohira A, Kunitake M. *Materials.* 2010; 3:4252–4276.
88. Dorokhin D, Hsu SH, Tomczak N, Reinhoudt DN, Huskens J, Velders AH, Vancso GJ. *ACS Nano.* 2010; 4:137–142. [PubMed: 20020751]

89. Gonzalez-Campo A, Hsu SH, Puig L, Huskens J, Reinhoudt DN, Velders AH. *J Am Chem Soc.* 2010; 132:11434–11436. [PubMed: 20677748]
90. Hu WS, Tao YT, Hsu YJ, Wei DH, Wu YS. *Langmuir.* 2005; 21:2260–2266. [PubMed: 15752014]
91. Clegg RS, Reed SM, Hutchison JE. *J Am Chem Soc.* 1998; 120:2486–2487.
92. Mao X, Wang Y, Liu L, Niu L, Yang Y, Wang C. *Langmuir.* 2009; 25:8849–8853. [PubMed: 19624165]
93. Nowinski AK, Sun F, White AD, Keefe AJ, Jiang S. *J Am Chem Soc.* 2012; 134:6000–6005. [PubMed: 22401132]
94. Prato M, Toccafondi C, Maidecchi G, Chaudhari V, Harish MNK, Sampath S, Parodi R, Esaulov VA, Canepa M. *J Phys Chem C.* 2012; 116:2431–2437.
95. Chaudhari V, Kotresh HMN, Srinivasan S, Esaulov VA. *J Phys Chem C.* 2011; 115:16518–16523.
96. Choi J-S, Kang H-G, Ito E, Hara M, Noh J-G. *Bull Kor Chem Soc.* 2011; 32:2623–2627.
97. Monnell JD, Stapleton JJ, Dirk SM, Reinert WA, Tour JM, Allara DL, Weiss PS. *J Phys Chem B.* 2005; 109:20343–20349. [PubMed: 16853632]
98. Szelagowska-Kunzman K, Cyganik P, Schupbach B, Terfort A. *Phys Chem Chem Phys.* 2010; 12:4400–4406. [PubMed: 20407712]
99. Livage J. *J Solid State Chem.* 1986; 64:322–330.
100. Sanchez C, Boissière C, Grosso D, Laberty C, Nicole L. *Chem Mater.* 2008; 20:682–737.
101. Petrović, Ze; Katić, J.; Metikoš-Huković, M.; Dadafarin, H.; Omanović, S. *J Electrochem Soc.* 2011; 158:F159–F165.
102. Baber AE, Lawton TJ, Sykes ECH. *J Phys Chem C.* 2011; 115:9157–9163.
103. Otero R, Rosei F, Besenbacher F. *Annu Rev Phys Chem.* 2006; 57:497–525. [PubMed: 16599819]
104. Baber AE, Jensen SC, Sykes EC. *J Am Chem Soc.* 2007; 129:6368–6369. [PubMed: 17472383]
105. Han P, Weiss PS. *Surf Sci Rep.* 2012; 67:19–81.
106. Yan L, Zheng YB, Zhao F, Li S, Gao X, Xu B, Weiss PS, Zhao Y. *Chem Soc Rev.* 2012; 41:97–114. [PubMed: 22086617]
107. Arakawa H, Umemura K, Ikai A. *Nature.* 1992; 358:171–173. [PubMed: 1377369]
108. Mao X, Wang C, Ma X, Zhang M, Liu L, Zhang L, Niu L, Zeng Q, Yang Y. *Nanoscale.* 2011; 3:1592–1599. [PubMed: 21283870]
109. Torres E, Blumenau AT, Biedermann PU. *Chemphyschem.* 2011; 12:999–1009. [PubMed: 21394869]
110. Poirier GE. *J Vac Sci Technol B.* 1996; 14:1453–1460.
111. Moore AM, Yeganeh S, Yao Y, Claridge SA, Tour JM, Ratner MA, Weiss PS. *ACS Nano.* 2010; 4:7630–7636. [PubMed: 21077677]
112. Clegg RS, Hutchison JE. *J Am Chem Soc.* 1999; 121:5319–5327.
113. Lewis PA, Smith RK, Kelly KF, Bumm LA, Reed SM, Clegg RS, Gunderson JD, Hutchison JE, Weiss PS. *J Phys Chem B.* 2001; 105:10630–10636.
114. Yoon HJ, Shapiro ND, Park KM, Thuo MM, Soh S, Whitesides GM. *Angew Chem Int Ed Engl.* 2012; 51:4658–4661. [PubMed: 22504880]
115. Smith RK, Reed SM, Lewis PA, Monnell JD, Clegg RS, Kelly KF, Bumm LA, Hutchison JE, Weiss PS. *J Phys Chem B.* 2001; 105:1119–1122.
116. Kim M, Hohman JN, Serino AC, Weiss PS. *J Phys Chem C.* 2010; 114:19744–19751.
117. Grave C, Risko C, Shaporenko A, Wang Y, Nuckolls C, Ratner MA, Rampi MA, Zharnikov M. *Adv Funct Mater.* 2007; 17:3816–3828.
118. Donhauser ZJ, Mantooth BA, Kelly KF, Bumm LA, Monnell JD, Stapleton JJ, Price DW, Rawlett AM, Allara DL, Tour JM, Weiss PS. *Science.* 2001; 292:2303–2307. [PubMed: 11423655]
119. Vaish A, Shuster MJ, Cheunkar S, Singh YS, Weiss PS, Andrews AM. *ACS Chem Neurosci.* 2010; 1:495–504. [PubMed: 22778841]
120. Geyer W, Stadler V, Eck W, Zharnikov M, Golzhauser A, Grunze M. *Appl Phys Lett.* 1999; 75:2401–2403.

121. Chabinye ML, Chen XX, Holmlin RE, Jacobs H, Skulason H, Frisbie CD, Mujica V, Ratner MA, Rampi MA, Whitesides GM. *J Am Chem Soc.* 2002; 124:11730–11736. [PubMed: 12296740]
122. Bould J, Machacek J, Londesborough MG, Macias R, Kennedy JD, Bastl Z, Rupper P, Base T. *Inorg Chem.* 2012; 51:1685–1694. [PubMed: 22229807]
123. Kim M, Hohman JN, Morin EI, Daniel TA, Weiss PS. *J Phys Chem A.* 2009; 113:3895–3903. [PubMed: 19309101]
124. Jobbins MM, Raigoza AF, Kandel SA. *J Phys Chem C.* 2011; 115:25437–25441.
125. Willey TM, Fabbri JD, Lee JRI, Schreiner PR, Rokin AA, Tkachenko BA, Fokina NA, Dahl JEP, Carlson RMK, Vance AL, Yang WJ, Terminello LJ, van Buuren T, Melosh NA. *J Am Chem Soc.* 2008; 130:10536–10544. [PubMed: 18642809]
126. Wang YY, Kioupakis E, Lu XH, Wegner D, Yamachika R, Dahl JE, Carlson RMK, Louie SG, Crommie MF. *Nat Mater.* 2008; 7:38–42. [PubMed: 18037893]
127. Hohman JN, Zhang P, Morin EI, Han P, Kim M, Kurland AR, McClanahan PD, Balema VP, Weiss PS. *ACS Nano.* 2009; 3:527–536. [PubMed: 19243128]
128. Wang H, He Y, Ratner BD, Jiang S. *J Biomed Mater Res A.* 2006; 77:672–678. [PubMed: 16514600]
129. Lee SH, Lin WC, Chang CJ, Huang CC, Liu CP, Kuo CH, Chang HY, You YW, Kao WL, Yen GJ, Kuo DY, Kuo YT, Tsai MH, Shyue JJ. *Phys Chem Chem Phys.* 2011; 13:4335–4339. [PubMed: 21258709]
130. Romaner L, Heimel G, Zojer E. *Phys Rev B.* 2008; 77:045113.
131. Carot ML, Macagno VA, Paredes-Olivera P, Patrio EM. *J Phys Chem C.* 2007; 111:4294–4304.
132. Watcharinyanon S, Moons E, Johansson LSO. *J Phys Chem C.* 2009; 113:1972–1979.
133. Chambers RC, Inman CE, Hutchison JE. *Langmuir.* 2005; 21:4615–4621. [PubMed: 16032880]
134. Yagüe JL, Agulló N, Fonder G, Delhalle J, Mekhalif Z, Borrós S. *Plasma Proc Pol.* 2010; 7:601–609.
135. Patnaik A, Setoyama H, Ueno N. *J Chem Phys.* 2004; 120:6214–6221. [PubMed: 15267508]
136. Shuster MJ, Vaish A, Szapacs ME, Anderson ME, Weiss PS, Andrews AM. *Adv Mater.* 2008; 20:164–167.
137. Shuster MJ, Vaish A, Cao HH, Guttentag AI, McManigle JE, Gibb AL, Martinez MM, Nezarati RM, Hinds JM, Liao WS, Weiss PS, Andrews AM. *Chem Comm.* 2011; 47:10641–10643. [PubMed: 21874174]
138. Cho J, Berbil-Bautista L, Levy N, Poulsen D, Frechet JM, Crommie MF. *J Chem Phys.* 2010; 133:234707. [PubMed: 21186884]
139. Smith RK, Nanayakkara SU, Woehrlé GH, Pearl TP, Blake MM, Hutchison JE, Weiss PS. *J Am Chem Soc.* 2006; 128:9266–9267. [PubMed: 16848426]
140. Vaish A, Liao WS, Shuster MJ, Hinds JM, Weiss PS, Andrews AM. *Anal Chem.* 2011; 83:7451–7456. [PubMed: 21866911]
141. Shuster MJ, Vaish A, Gilbert ML, Martinez-Rivera M, Nezarati RM, Weiss PS, Andrews AM. *J Phys Chem C.* 2011; 115:24778–24787.
142. Saavedra HM, Thompson CM, Hohman JN, Crespi VH, Weiss PS. *J Am Chem Soc.* 2009; 131:2252–2259. [PubMed: 19170497]
143. Perez-Luna VH, O'Brien MJ, Opperman KA, Hampton PD, Lopez GP, Klumb LA, SPS. *J Am Chem Soc.* 1999; 121:6469–6478.
144. Lahiri J, Ostuni E, Whitesides GM. *Langmuir.* 1999; 15:2055–2060.
145. Mrksich M. *ACS Nano.* 2008; 2:7–18. [PubMed: 19206542]
146. Weck M, Jackiw JJ, Rossi RR, Weiss PS, Grubbs RH. *J Am Chem Soc.* 1999; 121.
147. Lahiri J, Isaacs L, Tien J, Whitesides GM. *Anal Chem.* 1999; 71:777–790. [PubMed: 10051846]
148. Vaish A, Shuster MJ, Cheunkar S, Weiss PS, Andrews AM. *Small.* 2011; 7:1471–1479. [PubMed: 21538866]
149. Kolb HC, Finn MG, Sharpless KB. *Angew Chem-Int Edit.* 2001; 40:2004–2021.
150. Sun XL, Stabler CL, Cazalis CS, Chaikof EL. *Bioconj Chem.* 2006; 17:52–57.

151. Qin GT, Santos C, Zhang W, Li Y, Kumar A, Erasquin UJ, Liu K, Muradov P, Trautner BW, Cai CZ. *J Am Chem Soc.* 2010; 132:16432–16441. [PubMed: 21033708]
152. Paxton WF, Spruell JM, Stoddart JF. *J Am Chem Soc.* 2009; 131:6692–6694. [PubMed: 19388653]
153. Grim PCM, De Feyter S, Gesquiere A, Vanoppen P, Rucker M, Valiyaveetil S, Moessner G, Mullen K, De Schryver FC. *Angew Chem-Int Edit.* 1997; 36:2601–2603.
154. Akai-Kasaya M, Shimizu K, Watanabe Y, Saito A, Aono M, Kuwahara Y. *Phys Rev Lett.* 2003; 91:255501. [PubMed: 14754124]
155. Bensimon A, Simon A, Chiffaudel A, Croquette V, Heslot F, Bendimon D. *Science.* 1994; 265:2096–2098. [PubMed: 7522347]
156. Patolsky F, Weizmann Y, Willner I. *Nat Mater.* 2004; 3:692–695. [PubMed: 15359342]
157. Juluri BK, Kumar AS, Liu Y, Ye T, Yang YW, Flood AH, Fang L, Stoddart JF, Weiss PS, Huang TJ. *ACS Nano.* 2009; 3:291–300. [PubMed: 19236063]
158. Li DB, Paxton WF, Baughman RH, Huang TJ, Stoddart JF, Weiss PS. *MRS Bull.* 2009; 34:671–681.
159. Kumpf C, Marks LD, Ellis D, Smilgies D, Landemark E, Nielsen M, Feidenhans R, Zegenhagen J, Bunk O, Zeysing JH, Su Y, Johnson RL. *Phys Rev Lett.* 2001; 86:3586–3589. [PubMed: 11328029]
160. Besenbacher F. *Rep Prog Phys.* 1996; 59:1737–1802.
161. Eigler DM, Schweizer EK. *Nat Chem.* 1990; 344:524–526.
162. Hasegawa S, Avouris P. *Phys Rev Lett.* 1993; 71:1071–1074. [PubMed: 10055441]
163. Stranick SJ, Kamna MM, Weiss PS. *Science.* 1994; 266:99–102. [PubMed: 17814004]
164. Gambardella P, Dallmeyer A, Maiti K, Malagoli MC, Eberhardt W, Kern K, Carbone C. *Nature.* 2002; 416:301–304. [PubMed: 11907571]
165. Ising E. *Z Phys.* 1925; 31:253–258.
166. Bethe H. *Z Phys.* 1931; 71:205–226.
167. Kamna MM, Stranick SJ, Weiss PS. *Isr J Chem.* 1996; 36:59–62.
168. Schiffrin A, Riemann A, Auwarter W, Pennec Y, Weber-Bargioni A, Cvetko D, Cossaro A, Morgante A, Barth JV. *Proc Natl Acad Sci U S A.* 2007; 104:5279–5284. [PubMed: 17372212]
169. Pennec Y, Auwarter W, Schiffrin A, Weber-Bargioni A, Riemann A, Barth JV. *Nat Nano.* 2007; 2:99–103.
170. Coskun A, Banaszak M, Astumian RD, Stoddart JF, Grzybowski BA. *Chem Soc Rev.* 2012; 41:19–30. [PubMed: 22116531]
171. Ye T, Kumar AS, Saha S, Takami T, Huang TJ, Stoddart JF, Weiss PS. *ACS Nano.* 2010; 4:3697–3701. [PubMed: 20540555]
172. Huang TJ, Brough B, Ho CM, Liu Y, Flood AH, Bonvallet PA, Tseng HR, Stoddart JF, Baller M, Magonov S. *Appl Phys Lett.* 2004; 85:5391–5393.
173. Rothmund PWK. *Nature.* 2006; 440:297–302. [PubMed: 16541064]
174. Gu HZ, Chao J, Xiao SJ, Seeman NC. *Nature.* 2010; 465:202–205. [PubMed: 20463734]
175. Wilner OI, Willner I. *Chem Rev.* 2012; 112:2528–2556. [PubMed: 22233123]
176. Mao X-B, Wang C-X, Wu X-K, Ma X-J, Liu L, Zhang L, Niu L, Guo Y-Y, Li D-H, Yang Y-L, Wang C. *Proc Natl Acad Sci U S A.* 2011; 108:19605–19610. [PubMed: 22106265]
177. Wei YH, Tong WJ, Zimmt MB. *J Am Chem Soc.* 2008; 130:3399–3405. [PubMed: 18302370]
178. Cyr DM, Venkataraman B, Flynn GW. *Chem Mater.* 1996; 8:1600–1615.
179. Cyr DM, Venkataraman B, Flynn GW, Black A, Whitesides GM. *J Phys Chem.* 1996; 100:13747–13759.
180. Takami K, Kuwahara Y, Ishii T, Akai-Kasaya M, Saito A, Aono M. *Surf Sci.* 2005; 591:L273–L279.
181. Okawa Y, Aono M. *J Chem Phys.* 2001; 115:2317–2322.
182. Scott JC, Samuel JDJ, Hou JH, Rettner CT, Miller RD. *Nano Lett.* 2006; 6:2916–2919. [PubMed: 17163730]
183. Joachim C, Gimzewski JK, Aviram A. *Nature.* 2000; 408:541–548. [PubMed: 11117734]

184. Moth-Poulsen K, Bjornholm T. *Nat Nano*. 2009; 4:551–556.
185. Aviram A, Ratner MA. *Chem Phys Lett*. 1974; 29:277–283.
186. Metzger RM. *J Mater Chem*. 2008; 18:4364–4396.
187. McCreery RL, Bergren AJ. *Adv Mater*. 2009; 21:4303–4322.
188. Heath JR, Ratner MA. *Phys Today*. 2003; 56:43–49.
189. Joachim C, Magoga M. *Chem Phys*. 2002; 281:347–352.
190. Gimzewski JK, Joachim C. *Science*. 1999; 283:1683–1688. [PubMed: 10073926]
191. Moore AM, Weiss PS. *Annu Rev Anal Chem*. 2008; 1:857–882.
192. Chen F, Tao NJ. *Acc Chem Res*. 2009; 42:429–438. [PubMed: 19253984]
193. Lewis PA, Inman CE, Yao YX, Tour JM, Hutchison JE, Weiss PS. *J Am Chem Soc*. 2004; 126:12214–12215. [PubMed: 15453724]
194. Donhauser ZJ, Price DW, Tour JM, Weiss PS. *J Am Chem Soc*. 2003; 125:11462–11463. [PubMed: 13129325]
195. Krans JM, Vanruijtenbeek JM, Fisun VV, Yanson IK, Dejongh LJ. *Nature*. 1995; 375:767–769.
196. Nielsen SK, Noat Y, Brandbyge M, Smit RHM, Hansen K, Chen LY, Yanson AI, Besenbacher F, van Ruitenbeek JM. *Phys Rev B*. 2003; 67:245411.
197. Qin L, Park S, Huang L, Mirkin CA. *Science*. 2005; 308:113–115. [PubMed: 15994551]
198. Lorente N, Persson M, Lauhon LJ, Ho W. *Phys Rev Lett*. 2001; 86:2593–2596. [PubMed: 11289988]
199. Lauhon LJ, Ho W. *Phys Rev B*. 1999; 60:R8525–R8528.
200. Reed MA, Zhou C, Muller CJ, Burgin TP, Tour JM. *Science*. 1997; 278:252–254.
201. Selzer Y, Cabassi MA, Mayer TS, Allara DL. *J Am Chem Soc*. 2004; 126:4052–4053. [PubMed: 15053563]
202. Chen F, Hihath J, Huang ZF, Li XL, Tao NJ. *Annu Rev Phys Chem*. 2007; 58:535–564. [PubMed: 17134372]
203. Xue YQ, Datta S, Ratner MA. *J Chem Phys*. 2001; 115:4292–4299.
204. Xue Y, Ratner MA. *Phys Rev B*. 2003; 68:115406.
205. Xu BQ, Tao NJ. *Science*. 2003; 301:1221–1223. [PubMed: 12947193]
206. Lindsay SM, Ratner MA. *Adv Mater*. 2007; 19:23–31.
207. Park YS, Whalley AC, Kamenetska M, Steigerwald ML, Hybertsen MS, Nuckolls C, Venkataraman L. *J Am Chem Soc*. 2007; 129:15768–15769. [PubMed: 18052282]
208. Chen F, Li XL, Hihath J, Huang ZF, Tao NJ. *J Am Chem Soc*. 2006; 128:15874–15881. [PubMed: 17147400]
209. Pathem BK, Claridge SA, Zheng YB, Weiss PS. *Annu Rev Phys Chem*. 2013; 64 in press. 10.1146/ANNUREV-PHYSCHEM-040412-110045
210. Metzger RM. *Chem Rev*. 2003; 103:3803–3834. [PubMed: 12964885]
211. Geddes NJ, Sambles JR, Jarvis DJ, Parker WG, Sandman DJ. *Appl Phys Lett*. 1990; 56:1916–1918.
212. Geddes NJ, Sambles JR, Jarvis DJ, Parker WG, Sandman DJ. *J Appl Phys*. 1992; 71:756–768.
213. Krzeminski C, Delerue C, Allan G, Vuillaume D, Metzger RM. *Phys Rev B*. 2001; 64:085405.
214. Metzger RM, Xu T, Peterson IR. *J Phys Chem B*. 2001; 105:7280–7290.
215. Ashwell GJ, Urasinska B, Tyrrell WD. *Phys Chem Chem Phys*. 2006; 8:3314–3319. [PubMed: 16835679]
216. Donhauser ZJ, Mantooth BA, Pearl TP, Kelly KF, Nanayakkara SU, Weiss PS. *Japan J Appl Phys*. 2002; 41:4871–4877.
217. Zhou XL, Zhu XY, White JM. *Surf Sci Rep*. 1991; 13:73–220.
218. Comstock MJ, Levy N, Kirakosian A, Cho JW, Lauterwasser F, Harvey JH, Strubbe DA, Frechet MJJ, Trauner D, Louie SG, Crommie MF. *Phys Rev Lett*. 2007; 99:038301. [PubMed: 17678335]
219. Comstock MJ, Levy N, Cho J, Berbil-Bautista L, Crommie MF, Poulsen DA, Frechet MJJ. *Appl Phys Lett*. 2008; 92:123107.

220. Hagen S, Kale P, Leyssner F, Nandi D, Wolf M, Tegeder P. *J Chem Phys.* 2008; 129:164102. [PubMed: 19045242]
221. Pathem BK, Zheng YB, Payton JL, Song T-B, Yu B-C, Tour JM, Jensen YYL, Weiss PS. *J Phys Chem Lett.* 2012; 3:2388–2394.
222. Davis JJ, Orłowski GA, Rahman H, Beer PD. *Chem Comm.* 2010; 46:54–63. [PubMed: 20024293]
223. Collier CP, Mattersteig G, Wong EW, Luo Y, Beverly K, Sampaio J, Raymo FM, Stoddart JF, Heath JR. *Science.* 2000; 289:1172–1175. [PubMed: 10947980]
224. Stoddart JF. *Chem Soc Rev.* 2009; 38:1802–1820. [PubMed: 19587969]
225. Coskun A, Spruell JM, Barin G, Dichtel WR, Flood AH, Botros YY, Stoddart JF. *Chem Soc Rev.* 2012; 41:4827–4859. [PubMed: 22648395]
226. Mayne AJ, Dujardin G, Comtet G, Riedel D. *Chem Rev.* 2006; 106:4355–4378. [PubMed: 17031990]
227. Lauhon LJ, Ho W. *J Phys Chem A.* 2000; 104:2463–2467.
228. Hla SW, Bartels L, Meyer G, Rieder KH. *Phys Rev Lett.* 2000; 85:2777–2780. [PubMed: 10991231]
229. Blake MM, Nanayakkara SU, Claridge SA, Fernandez-Torres LC, Sykes ECH, Weiss PS. *J Phys Chem A.* 2009; 113:13167–13172. [PubMed: 19658380]
230. Kim M, Hohman JN, Cao Y, Houk KN, Ma H, Jen AK, Weiss PS. *Science.* 2011; 331:1312–1315. [PubMed: 21393542]
231. Bustamante C, Macosko JC, Wuite GJL. *Nat Rev Mol Cell Biol.* 2000; 1:130–136. [PubMed: 11253365]
232. Kelley AM, Michalet X, Weiss S. *Science.* 2001; 292:1671–1672. [PubMed: 11387465]
233. Greenleaf WJ, Woodside MT, Block SM. *Annu Rev Biophys Biomol Struct.* 2007; 36:171–190. [PubMed: 17328679]
234. Harpaz Y, Gerstein M, Chothia C. *Structure.* 1994; 2:641–649. [PubMed: 7922041]
235. Srinivasan C, Mullen TJ, Hohman JN, Anderson ME, Dameron AA, Andrews AM, Dickey EC, Horn MW, Weiss PS. *ACS Nano.* 2007; 1:191–201. [PubMed: 19206649]
236. Bain CD, Troughton EB, Tao YT, Evall J, Whitesides GM, Nuzzo RG. *J Am Chem Soc.* 1989; 111:321–335.
237. Xia YN, Kim E, Whitesides GM. *J Electrochem Soc.* 1996; 143:1070–1079.
238. Xia YN, Venkateswaran N, Qin D, Tien J, Whitesides GM. *Langmuir.* 1998; 14:363–371.
239. Xia YN, Kim E, Mrksich M, Whitesides GM. *Chem Mater.* 1996; 8:601–603.
240. Carvalho A, Geissler M, Schmid H, Michel B, Delamarche E. *Langmuir.* 2002; 18:2406–2412.
241. Heinemann N, Grunau J, Leissner T, Andreyev O, Kuhn S, Jung U, Zargarani D, Herges R, Magnussen O, Bauer M. *Chem Phys.* 2012; 402:22–28.
242. Pechenezhskiy IV, Cho J, Nguyen GD, Berbil-Bautista L, Giles BL, Poulsen DA, Frechet JMJ, Crommie MF. *J Phys Chem C.* 2012; 116:1052–1055.
243. Lee TR, Laibinis PE, Folkers JP, Whitesides GM. *Pure Appl Chem.* 1991; 63:821–828.
244. Solanki PR, Prabhakar N, Pandey MK, Malhotra BD. *Biomed Microdevices.* 2008; 10:757–767. [PubMed: 18574694]
245. Balamurugan S, Obubuafo A, Soper SA, McCarley RL, Spivak DA. *Langmuir.* 2006; 22:6446–6453. [PubMed: 16800712]
246. Jans K, Bonroy K, De Palma R, Reekmans G, Jans H, Laureyn W, Smet M, Borghs G, Maes G. *Langmuir.* 2008; 24:3949–3954. [PubMed: 18315018]
247. Chaki NK, Vijayamohan K. *Biosens Bioelectron.* 2002; 17:1–12. [PubMed: 11742729]
248. Kumar A, Biebuyck HA, Whitesides GM. *Langmuir.* 1994; 10:1498–1511.
249. Xia YN, Whitesides GM. *Annu Rev Mater Sci.* 1998; 28:153–184.
250. Xia YN, Rogers JA, Paul KE, Whitesides GM. *Chem Rev.* 1999; 99:1823–1848. [PubMed: 11849012]
251. Piner RD, Zhu J, Xu F, Hong SH, Mirkin CA. *Science.* 1999; 283:661–663. [PubMed: 9924019]
252. Tseng AA, Notargiacomo A, Chen TP. *J Vac Sci Technol B.* 2005; 23:877–894.



253. Ruiz SA, Chen CS. *Soft Matter*. 2007; 3:168–177.
254. Kumar A, Whitesides GM. *Appl Phys Lett*. 1993; 63:2002–2004.
255. Jackman RJ, Wilbur JL, Whitesides GM. *Science*. 1995; 269:664–666. [PubMed: 7624795]
256. Xia YN, Zhao XM, Kim E, Whitesides GM. *Chem Mater*. 1995; 7:2332–2337.
257. Xia YN, Zhao XM, Whitesides GM. *Microelectron Eng*. 1996; 32:255–268.
258. Chapman RG, Ostuni E, Yan L, Whitesides GM. *Langmuir*. 2000; 16:6927–6936.
259. Roberts C, Chen CS, Mrksich M, Martichonok V, Ingber DE, Whitesides GM. *J Am Chem Soc*. 1998; 120:6548–6555.
260. Lokanathan AR, Zhang S, Regina VR, Cole MA, Ogaki R, Dong MD, Besenbacher F, Meyer RL, Kingshott P. *Biointerphases*. 2011; 6:180–188. [PubMed: 22239811]
261. Chen CS, Mrksich M, Huang S, Whitesides GM, Ingber DE. *Science*. 1997; 276:1425–1428. [PubMed: 9162012]
262. Whitesides GM, Ostuni E, Takayama S, Jiang XY, Ingber DE. *Annu Rev Biomed Eng*. 2001; 3:335–373. [PubMed: 11447067]
263. Delamarche E, Schmid H, Bietsch A, Larsen NB, Rothuizen H, Michel B, Biebuyck H. *J Phys Chem B*. 1998; 102:3324–3334.
264. Mullen TJ, Srinivasan C, Shuster MJ, Horn MW, Andrews AM, Weiss PS. *J Nanopart Res*. 2008; 10:1231–1240.
265. Dameron AA, Hampton JR, Gillmor SD, Hohman JN, Weiss PS. *J Vac Sci Technol B*. 2005; 23:2929–2932.
266. Liebau M, Huskens J, Reinhoudt DN. *Adv Funct Mater*. 2001; 11:147–150.
267. Li HW, Muir BVO, Fichet G, Huck WTS. *Langmuir*. 2003; 19:1963–1965.
268. Balmer TE, Schmid H, Stutz R, Delamarche E, Michel B, Spencer ND, Wolf H. *Langmuir*. 2005; 21:622–632. [PubMed: 15641832]
269. Liebau M, Janssen HM, Inoue K, Shinkai S, Huskens J, Sijbesma RP, Meijer EW, Reinhoudt DN. *Langmuir*. 2002; 18:674–682.
270. Dameron AA, Hampton JR, Smith RK, Mullen TJ, Gillmor SD, Weiss PS. *Nano Lett*. 2005; 5:1834–1837. [PubMed: 16159233]
271. Mullen TJ, Srinivasan C, Hohman JN, Gillmor SD, Shuster MJ, Horn MW, Andrews AM, Weiss PS. *Appl Phys Lett*. 2007; 90:063114.
272. Vericat C, Vela ME, Salvarezza RC. *Phys Chem Chem Phys*. 2005; 7:3258–3268. [PubMed: 16240039]
273. Shuster MJ, Vaish A, Szapacs ME, Anderson ME, Weiss PS, Andrews AM. *Adv Mater*. 2008; 20:164–165.
274. Wadu-Mesthrige K, Amro NA, Liu GY. *Scanning*. 2000; 22:380–388. [PubMed: 11145264]
275. Huo FW, Zheng ZJ, Zheng GF, Giam LR, Zhang H, Mirkin CA. *Science*. 2008; 321:1658–1660. [PubMed: 18703709]
276. Xia YN, Whitesides GM. *J Am Chem Soc*. 1995; 117:3274–3275.
277. McLellan JM, Geissler M, Xia YN. *J Am Chem Soc*. 2004; 126:10830–10831. [PubMed: 15339153]
278. Li XM, Peter M, Huskens J, Reinhoudt DN. *Nano Lett*. 2003; 3:1449–1453.
279. Wendeln C, Ravoo BJ. *Langmuir*. 2012; 28:5527–5538. [PubMed: 22263907]
280. Sullivan TP, van Poll ML, Dankers PYW, Huck WTS. *Angew Chem-Int Edit*. 2004; 43:4190–4193.
281. Mizuno H, Buriak JM. *J Am Chem Soc*. 2008; 130:17656–17657. [PubMed: 19063631]
282. Rozkiewicz DI, Janczewski D, Verboom W, Ravoo BJ, Reinhoudt DN. *Angew Chem-Int Edit*. 2006; 45:5292–5296.
283. Spruell JM, Sheriff BA, Rozkiewicz DI, Dichtel WR, Rohde RD, Reinhoudt DN, Stoddart JF, Heath JR. *Angew Chem-Int Edit*. 2008; 47:9927–9932.
284. Mizuno H, Buriak JM. *ACS Appl Mater Int*. 2009; 1:2711–2720.
285. Jang JY, Hong SH, Schatz GC, Ratner MA. *J Chem Phys*. 2001; 115:2721–2729.

286. Sheehan PE, Whitman LJ. *Phys Rev Lett*. 2002; 88:156104. [PubMed: 11955210]
287. Rozhok S, Piner R, Mirkin CA. *J Phys Chem B*. 2003; 107:751–757.
288. Lee KB, Park SJ, Mirkin CA, Smith JC, Mrksich M. *Science*. 2002; 295:1702–1705. [PubMed: 11834780]
289. Demers LM, Ginger DS, Park SJ, Li Z, Chung SW, Mirkin CA. *Science*. 2002; 296:1836–1838. [PubMed: 12052950]
290. Lee KB, Lim JH, Mirkin CA. *J Am Chem Soc*. 2003; 125:5588–5589. [PubMed: 12733870]
291. Noy A, Miller AE, Klare JE, Weeks BL, Woods BW, DeYoreo JJ. *Nano Lett*. 2002; 2:109–112.
292. Lim JH, Ginger DS, Lee KB, Heo J, Nam JM, Mirkin CA. *Angew Chem-Int Edit*. 2003; 42:2309–2312.
293. Zhang H, Chung SW, Mirkin CA. *Nano Lett*. 2003; 3:43–45.
294. Hyun J, Ahn SJ, Lee WK, Chilkoti A, Zauscher S. *Nano Lett*. 2002; 2:1203–1207.
295. Zhang H, Li Z, Mirkin CA. *Adv Mater*. 2002; 14:1472–1473.
296. Hampton JR, Dameron AA, Weiss PS. *J Phys Chem B*. 2005; 109:23118–23120. [PubMed: 16375269]
297. Hong SH, Mirkin CA. *Science*. 2000; 288:1808–1811. [PubMed: 10846159]
298. Zhang M, Bullen D, Chung SW, Hong S, Ryu KS, Fan ZF, Mirkin CA, Liu C. *Nanotechnology*. 2002; 13:212–217.
299. Salaita K, Wang YH, Fragala J, Vega RA, Liu C, Mirkin CA. *Angew Chem-Int Edit*. 2006; 45:7220–7223.
300. Mirkin CA. *ACS Nano*. 2007; 1:79–83. [PubMed: 19206523]
301. Liu GY, Xu S, Qian YL. *Acc Chem Res*. 2000; 33:457–466. [PubMed: 10913234]
302. Xu S, Liu GY. *Langmuir*. 1997; 13:127–129.
303. Amro NA, Xu S, Liu GY. *Langmuir*. 2000; 16:3006–3009.
304. Xu S, Miller S, Laibinis PE, Liu GY. *Langmuir*. 1999; 15:7244–7251.
305. Wadu-Mesthrige K, Xu S, Amro NA, Liu GY. *Langmuir*. 1999; 15:8580–8583.
306. Wadu-Mesthrige K, Amro NA, Garno JC, Xu S, Liu GY. *Biophys J*. 2001; 80:1891–1899. [PubMed: 11259301]
307. Tan YH, Liu M, Nolting B, Go JG, Gervay-Hague J, Liu GY. *ACS Nano*. 2008; 2:2374–2384. [PubMed: 19206405]
308. Xu S, Laibinis PE, Liu GY. *J Am Chem Soc*. 1998; 120:9356–9361.
309. Garcia R, Martinez RV, Martinez J. *Chem Soc Rev*. 2006; 35:29–38. [PubMed: 16365640]
310. Liu GY, Amro NA. *Proc Natl Acad Sci U S A*. 2002; 99:5165–5170. [PubMed: 11959965]
311. Josephs EA, Ye T. *J Am Chem Soc*. 2010; 132:10236–10238. [PubMed: 20662500]
312. Liu JF, Cruchon-Dupeyrat S, Garno JC, Frommer J, Liu GY. *Nano Lett*. 2002; 2:937–940.
313. Corbitt TS, Crooks RM, Ross CB, Hampdensmith MJ, Schoer JK. *Adv Mater*. 1993; 5:935–938.
314. Schoer JK, Crooks RM. *Langmuir*. 1997; 13:2323–2332.
315. Chen J, Reed MA, Asplund CL, Cassell AM, Myrick ML, Rawlett AM, Tour JM, Van Patten PG. *Appl Phys Lett*. 1999; 75:624–626.
316. Gorman CB, Carroll RL, He YF, Tian F, Fuierer R. *Langmuir*. 2000; 16:6312–6316.
317. Geissler M, McLellan JM, Xia YN. *Nano Lett*. 2005; 5:31–36. [PubMed: 15792408]
318. Geissler M, McLellan JM, Chen JY, Xia YN. *Angew Chem-Int Edit*. 2005; 44:3596–3600.
319. Geissler M, Chalsani P, Cameron NS, Veres T. *Small*. 2006; 2:760–765. [PubMed: 17193120]
320. Hatzor A, Weiss PS. *Science*. 2001; 291:1019–1020. [PubMed: 11161210]
321. Anderson ME, Tan LP, Tanaka H, Mihok M, Lee H, Horn MW, Weiss PS. *J Vac Sci Technol B*. 2003; 21:3116–3119.
322. Srinivasan C, Hohman JN, Anderson ME, Weiss PS, Horn MW. *J Vac Sci Technol B*. 2007; 25:1985–1988.
323. Subramanian S, Catchmark JM. *J Microlithogr Microfabr Microsyst*. 2006; 5:049701.

324. Subramanian S, McCarty GS, Catchmark JM. *J Microlithogr Microfabr Microsyst.* 2005; 4:049701.
325. Li CB, Hasegawa T, Tanaka H, Miyazaki H, Odaka S, Tsukagoshi K, Aono M. *Nanotechnology.* 2010; 21:495304. [PubMed: 21079291]
326. McCarty GS. *Nano Lett.* 2004; 4:1391–1394.
327. Johnson S, Evans D, Davies AG, Linfield EH, Walti C. *Nanotechnology.* 2009; 20:155304. [PubMed: 19420546]
328. Hino T, Tanaka H, Ozawa H, Lida Y, Ogawa T. *Colloid Surf A-Physicochem Eng Asp.* 2008; 313:369–372.
329. Negishi R, Hasegawa T, Terabe K, Aono M, Ebihara T, Tanaka H, Ogawa T. *Appl Phys Lett.* 2006; 88:223111.
330. Anderson ME, Mihok M, Tanaka H, Tan LP, Horn MW, McCarty GS, Weiss PS. *Adv Mater.* 2006; 18:1020–1021.
331. Anderson ME, Smith RK, Donhauser ZJ, Hatzor A, Lewis PA, Tan LP, Tanaka H, Horn MW, Weiss PS. *J Vac Sci Technol B.* 2002; 20:2739–2744.
332. Tanaka H, Anderson ME, Horn MW, Weiss PS. *Jpn J Appl Phys Part 2 -Lett Express Lett.* 2004; 43:L950–L953.
333. Anderson ME, Srinivasan C, Jayaraman R, Weiss PS, Horn MW. *Microelectron Eng.* 2005; 78–79:248–252.
334. Srinivasan C, Anderson ME, Jayaraman R, Weiss PS, Horn MW. *Microelectron Eng.* 2006; 83:1517–1520.
335. Yeom HW, Takeda S, Rotenberg E, Matsuda I, Horikoshi K, Schaefer J, Lee CM, Kevan SD, Ohta T, Nagao T, Hasegawa S. *Phys Rev Lett.* 1999; 82:4898–4901.
336. Liu M, Amro NA, Liu G-y. *Annu Rev Phys Chem.* 2008; 59:367–386. [PubMed: 18031212]
337. Williams JA, Gorman CB. *Langmuir.* 2007; 23:3103–3105. [PubMed: 17300207]

## Biographies

Shelley A. Claridge is a NIH Postdoctoral Fellow with Paul Weiss at UCLA. She completed her PhD in Chemistry at UC Berkeley in 2008 with Paul Alivisatos and Jean M. J. Fréchet, working on synthesis and bioconjugation of inorganic nanocrystals. From 1997 to 2003 she worked as a software engineer. She received a BS in Mathematics, Biochemistry, and Genetics from Texas A&M University in 1997. Her research interests are in single-molecule biological structure and biological-inorganic interfaces.



Wei-Ssu Liao received his BS degree from National Cheng Kung University, Taiwan, in 2000. In 2002, he received his MS from National Taiwan University, Taiwan. He received his PhD from Texas A&M University in 2009, working under the direction of Prof. Paul Cremer. He is currently a postdoctoral scholar working with Profs. Paul Weiss and Anne Andrews at UCLA. His research experience and interests lie in bioanalytical chemistry, surface chemistry, and plasmonic nanomaterials.

John C. Thomas obtained his BS at the University of Texas at San Antonio in 2008, while performing research in the field of palladium coordination chemistry in the lab of Prof.

Judith A. Walmsley. He is currently working towards his PhD with Prof. Paul Weiss at UCLA. His graduate research focuses on the scanning tunneling microscopy and spectroscopy of cage molecules for self-assembly, probing buried functionality of self-assembled systems, and extending the capabilities of the scanning tunneling microscope to make novel measurements at the molecular and atomic scales. This research is performed at low temperature (4 K), in extreme high vacuum, and also in catalytically relevant environments.

Yuxi Zhao obtained her BS in Macromolecular Science from Fudan University (China) in 2009 and wrote her diploma thesis in the field of inorganic-organic hybrid solar cells. She is currently pursuing her PhD in the Department of Chemistry at UCLA with Prof. Paul Weiss. Her research focuses on coupling photons to single molecules to guide the design of molecules for organic photovoltaics.

Huan H. Cao received his BS in Chemistry from Marshall University, Huntington, WV in 2008. His undergraduate research in the Norton Nanolaboratories focused on fabricating DNA constructs attached to Au nanodots on Si/SiO<sub>2</sub> surfaces, which can be used as templates for building bioelectronic devices. He is presently working toward his PhD degree with Profs. Paul Weiss and Anne Andrews. His research spans the physical and neural sciences, which include exploring unconventional molecular patterning techniques on solid substrates, investigating reaction mechanism at interfaces between molecular self-assembled monolayers and polymeric surfaces, and fabricating bioselective substrates capable of capturing and sorting biomolecules from complex media.

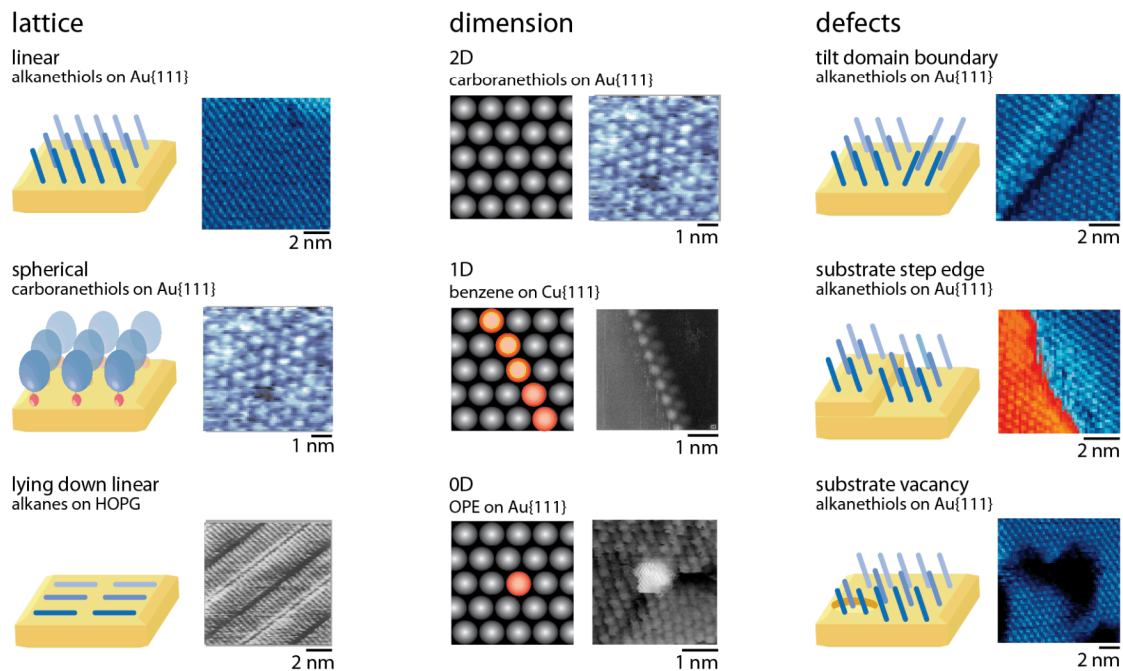
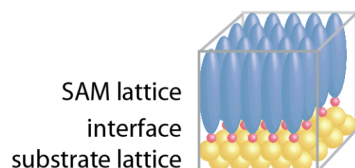
Sarawat Cheunkar graduated in 2004 with a BS in Chemistry from Mahidol University, Thailand. In 2005, he was awarded a full scholarship from the Ministry of Education, Royal Thai Government, to pursue his PhD working with Profs. Anne Andrews and Paul Weiss, first at the Pennsylvania State University, and currently at the California NanoSystems Institute at UCLA. He employs self-assembled monolayer techniques to develop neurotransmitter-functionalized surface chemistries. After completing his PhD, Mr. Cheunkar will join the faculty at the School of Bioresources and Technology, King Mongkut's University of Technology.

Andrew Serino received his BS from Penn State in 2010. His senior thesis was on characterizing intermolecular interactions in various self-assembled monolayers. He is currently pursuing a PhD in Materials Science and Engineering at the UCLA under the supervision of Prof. Paul Weiss. His research focus is on characterization of self-assembled materials and their utilization in devices.

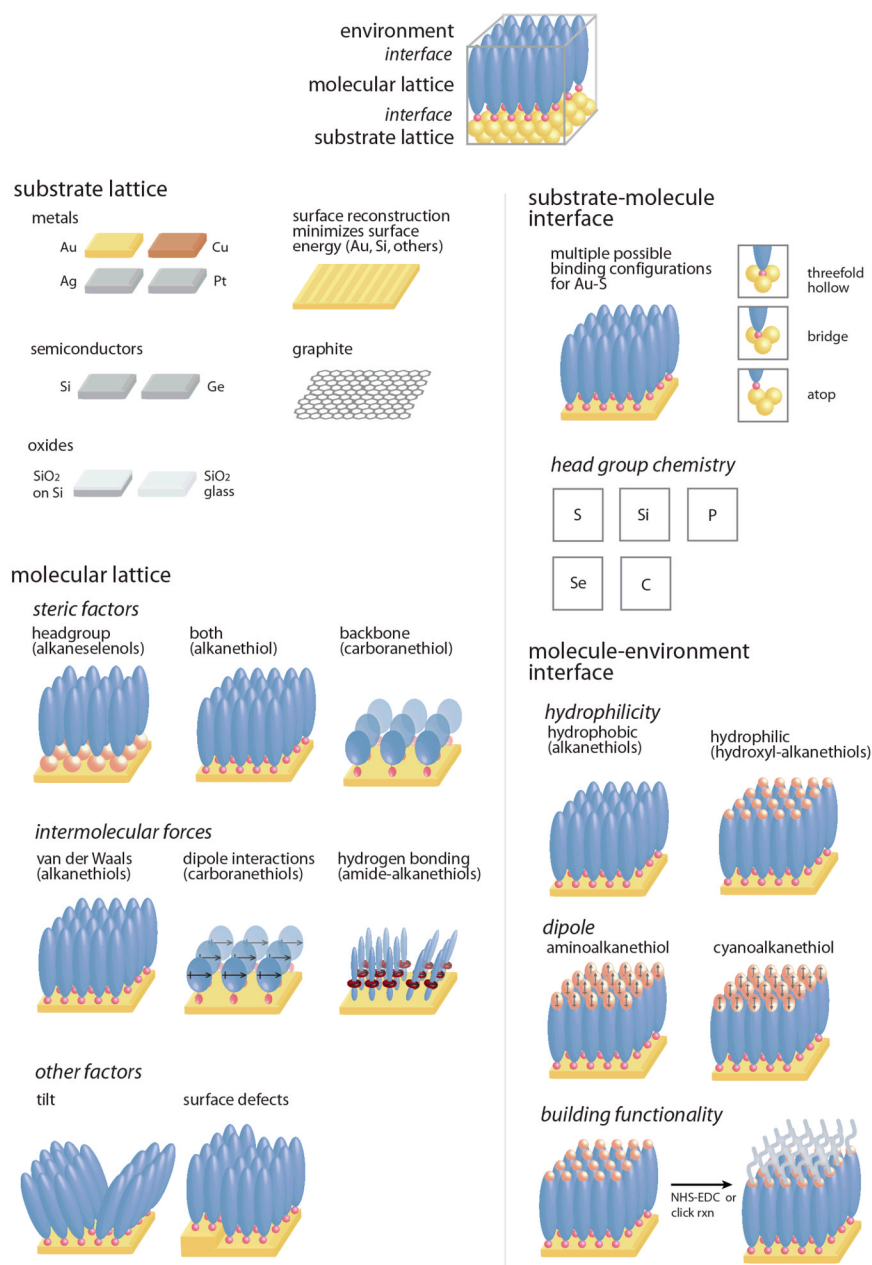
Anne Milasincic Andrews earned her PhD in Chemistry at the National Institute of Mental Health. At UCLA, she is a Professor of Psychiatry and Chemistry & Biochemistry, and a member of the Semel Institute for Neuroscience & Human Behavior, Hatos Center for Neuropharmacology, and California NanoSystems Institute. Among her awards are an Eli Lilly Outstanding Young Analytical Chemist Award, an American Parkinson's Disease Association Research Award, and a NARSAD Independent Investigator Award. She is an Associate Editor of *ACS Chemical Neuroscience*. Her basic and translational research interests focus on anxiety and depression, and at the nexus of nanoscience and neuroscience.

Paul S. Weiss received his PhD in Chemistry in 1986 from UC Berkeley. He was a postdoctoral fellow at AT&T Bell Laboratories and IBM Almaden Research Center. He began his academic career at Penn State, becoming Distinguished Professor of Chemistry and Physics before moving to UCLA in 2009. At UCLA, he is the Fred Kavli Chair in

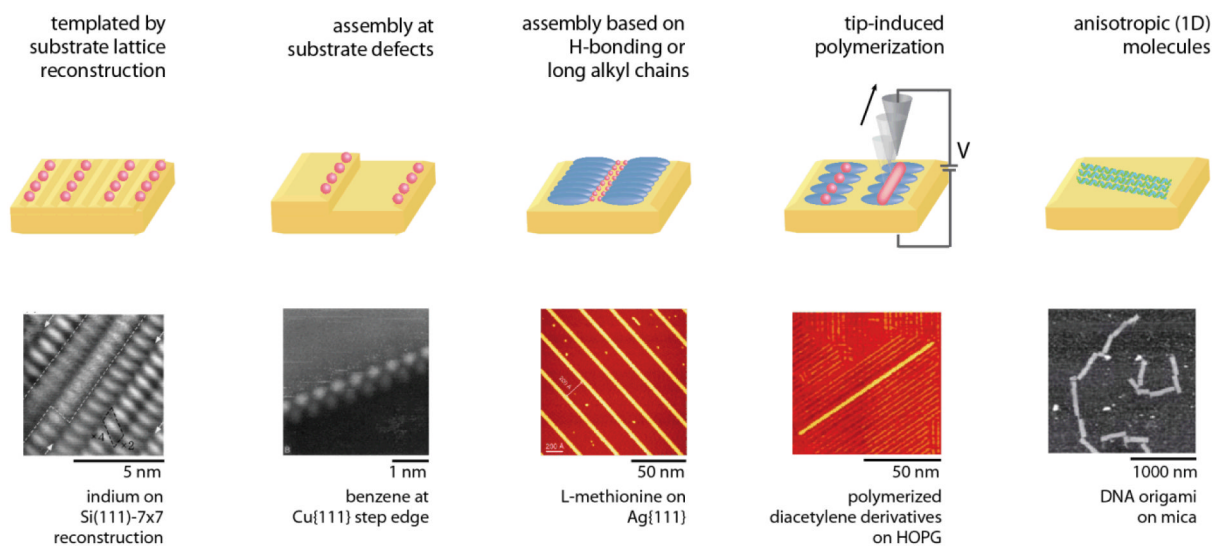
NanoSystems Sciences, the Director of the California NanoSystems Institute, and Distinguished Professor of Chemistry & Biochemistry and Materials Science & Engineering. He is the founding Editor-in-Chief of *ACS Nano*. His research interests are in single-molecule/assembly function, chemical patterning, self-assembly, and nanoscale analyses.



**Figure 1.** Self-assembled monolayers have molecular lattices that optimize interactions both with substrate lattices and between molecules in the monolayers, leading to a variety of lattice structures. Molecular structures in monolayers exhibit restricted dimensionality, similar to other nanostructured materials, which changes molecular behavior through directional coupling and other effects. Adapted with permission from refs. 19, 127, and 163. Defects in monolayer structure arise from substrate structure or molecular interactions, and create reactive sites in materials that can be used to control and to characterize molecular properties. Adapted with permission from ref. 12.

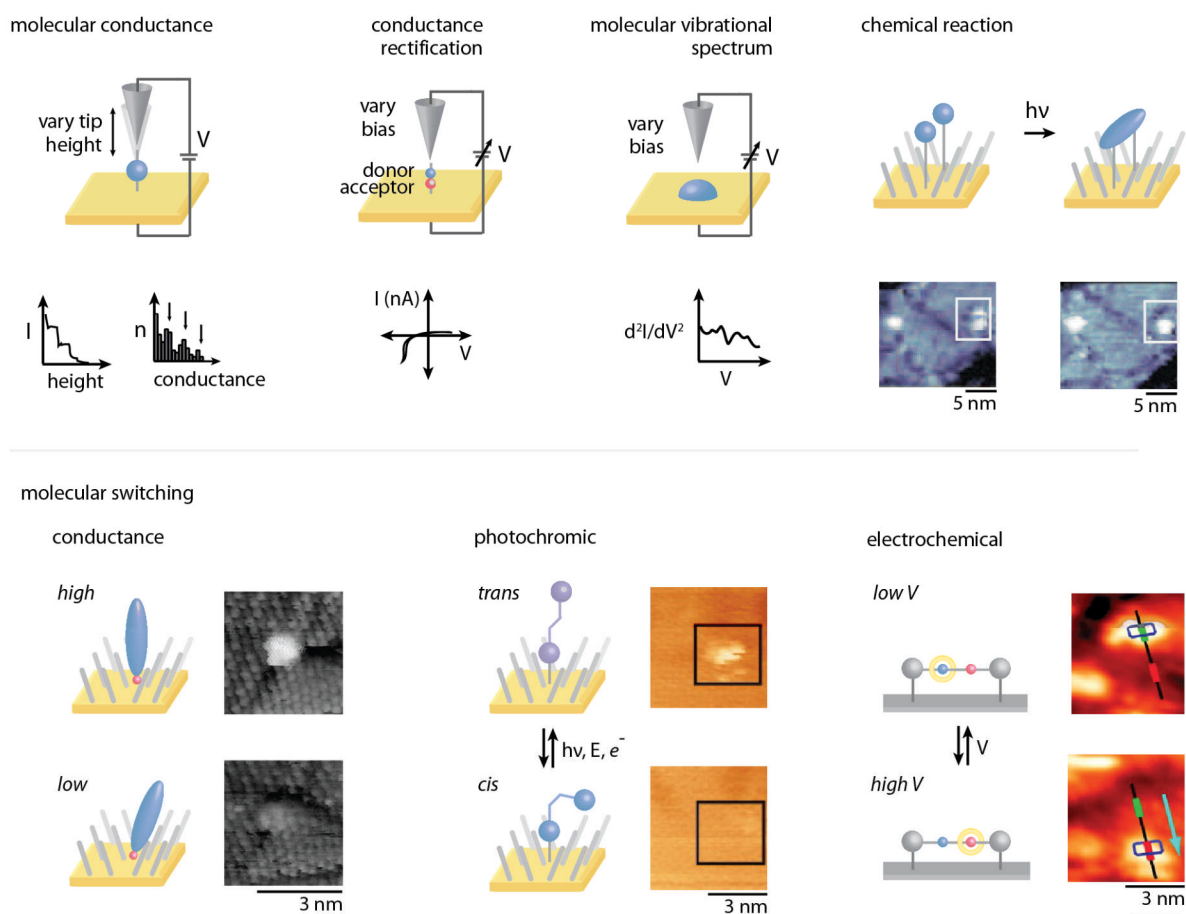


**Figure 2.** Two-dimensional molecular structures on surfaces form via the interplay between substrates and molecular lattices, and interactions at interfaces.

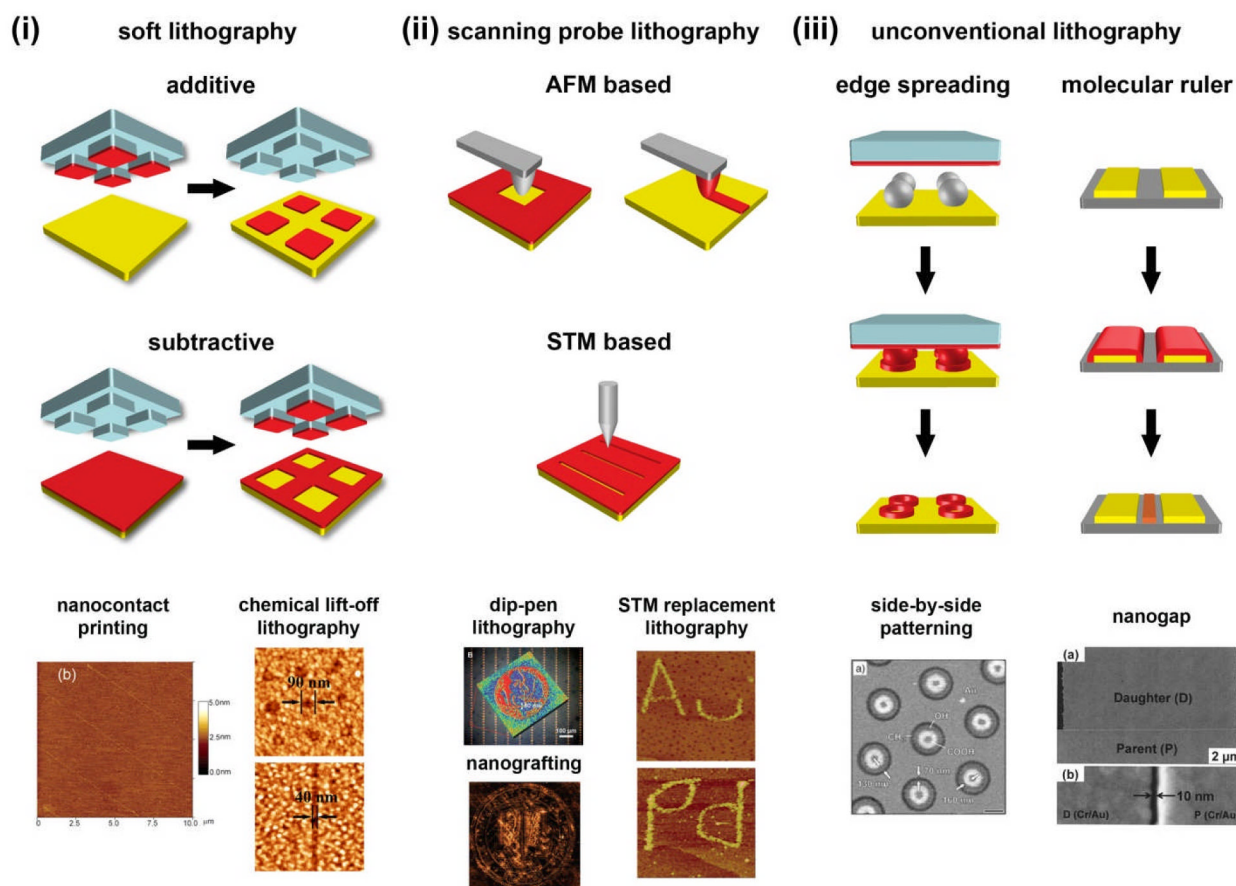


**Figure 3.** Strategies for 1D self-assembly. One-dimensional structures can be templated by substrates, either through anisotropic substrate lattices formed when substrates reconstruct to minimize surface energy, or at atomic step edges. One-dimensional structures can also be self-assembled from anisotropic molecules to form ordered assemblies due to interactions such as directional hydrogen-bonding or interactions between long alkyl chains. Such assemblies can then be polymerized to form covalently bound 1D structures. Finally, intrinsically 1D molecules such as DNA may be patterned on substrates directly. Adapted with permission from refs. 163, 168, 173, 181, and 335.





**Figure 4.** Molecular conductance is measured in a STM break junction by monitoring current as the STM probe tip is moved away from the surface (top left). A donor-bridge-acceptor molecular rectifier exhibits an asymmetric  $I$ - $V$  curve, also measured with STM (top center). Photodimerization of paired anthracene phenylene ethynylene derivatives isolated in a SAM is visualized with STM (top right). Adapted with permission from ref. 230. An isolated oligo(phenylene ethynylene) molecule inserted in a dodecanethiolate SAM on Au{111} undergoes reversible conductance switching (bottom left). Adapted with permission from ref. 19. Azobenzene inserted in a dodecanethiolate SAM undergoes reversible photoisomerization (bottom middle). Adapted with permission from ref. 15. The ring of a surface-bound rotaxane shuttles between two stations as the electrochemical potential in the cell is cycled from 0.1 V to 0.5 V (bottom right). Adapted with permission from ref. 171.

**Figure 5.**

Overview of molecular patterning strategies. (i) Soft lithography. Left: 42-nm lines of dendrimers on Si surfaces fabricated by additive nanocontact printing. Adapted with permission from ref. 267. Right: Biotin-streptavidin recognition patterns on Au substrates fabricated by subtractive chemical lift-off lithography. Adapted with permission from ref. 58. (ii) Scanning probe lithography. Left: Large-area patterning of 1-octadecanethiol with dip-pen nanolithography; and nanografting aldehyde-terminated thiols into decanethiol SAMs. Adapted with permission from refs. 299 and 336. Right: Replacement of dodecanethiol SAMs with ferrocenyl undecyl thioacetate molecules on Au and Pd substrates assisted by high-bias ( $>2$  V) scanning with STM probes. Adapted with permission from ref. 337. (iii) Unconventional lithography. Left: Side-by-side patterning for carboxy- (bright), hydroxy- (gray), and methyl-terminated (dark) thiolate monolayers on Au substrates. Adapted with permission from ref. 318. Right: A 10-nm gap fabricated by molecular ruler technique. Adapted with permission from ref. 322.